

Vertex nomination between graphs via spectral embedding and quadratic programming

Runbing Zheng

Department of Statistics, North Carolina State University

Vince Lyzinski*

Department of Mathematics, University of Maryland

Carey E. Priebe

Department of Applied Mathematics and Statistics, Johns Hopkins University

Minh Tang

Department of Statistics, North Carolina State University

May 30, 2022

Abstract

Given a network and a subset of interesting vertices whose identities are *only partially* known, the vertex nomination problem seeks to rank the remaining vertices in such a way that the interesting vertices are ranked at the top of the list. An important variant of this problem is vertex nomination in the multiple graphs setting. Given two graphs G_1, G_2 with common vertices and a vertex of interest $x \in G_1$, we wish to rank the vertices of G_2 such that the vertices most similar to x are ranked at the top of the list. The current paper addresses this problem and proposes a method that first applies adjacency spectral graph embedding to embed the graphs into a common Euclidean space, and then solves a penalized linear assignment problem to obtain the nomination lists. Since the spectral embedding of the graphs are only unique up to orthogonal transformations, we present two approaches to eliminate this potential non-identifiability. One approach is based on orthogonal Procrustes and is applicable when there are enough vertices with known correspondence between the two graphs. Another approach uses adaptive point set registration and is applicable

*This material is based on research sponsored by the Air Force Research Laboratory and DARPA under agreement number FA8750-20-2-1001. The U.S. Government is authorized to reproduce and distribute reprints for Governmental purposes notwithstanding any copyright notation thereon. The views and conclusions contained herein are those of the authors and should not be interpreted as necessarily representing the official policies or endorsements, either expressed or implied, of the Air Force Research Laboratory and DARPA or the U.S. Government.

when there are few or no vertices with known correspondence. We show that our nomination scheme leads to accurate nomination under a generative model for pairs of random graphs that are approximately low-rank and possibly with pairwise edge correlations. We illustrate our algorithm’s performance through simulation studies on synthetic data as well as analysis of a high-school friendship network and analysis of transition rates between web pages on the Bing search engine.

Keywords: vertex nomination, correlated graphs, generalized random dot product graphs, point set registration

1 Introduction

Graphs are widely used to model data in various fields wherein vertices represent entities or objects of interest and the edges represent pairwise relationships between the vertices. For example, in social network graphs the vertices represent individuals with the edges showing the communication between these individuals. Another example is citation network where the vertices represent articles and the (directed) edges represent citations between the articles. Finally, in many neuroscience applications, the vertices represent brain regions of interest and the edges summarize the inter-connectivity between these regions. Due to the prevalence of network data, there has been a great deal of research done recently in statistical inference on graphs, including, but not limited to, estimation of graph parameters, (Lloyd et al., 2012; Xu, 2017), one-sample and multi-sample hypothesis testing (Moreno and Neville, 2013; Tang et al., 2017), graph clustering and classification (Kudo et al., 2005; Schaeffer, 2007; Yin et al., 2017; Zhang et al., 2018), and vertex nomination (Fishkind et al., 2015; Yoder et al., 2020).

Vertex nomination is the graph analog of recommender systems for general tabular data. The simplest and most widely studied variant of this problem is in the single graph setting wherein, given a network and a subset of interesting vertices whose identities are partially known, the task is to identify, using the known interesting vertices, the remaining vertices of interest. The number of interesting vertices is, in general, much smaller than the total number of vertices in the graphs, and vertex nomination algorithms usually seek to output a list of candidate vertices (that are deemed interesting) with the aim that the remaining true but unknown vertices of interest are concentrated near the top of the list.

The vertex nomination problem in the single graph setting appears, at first blush, to be similar to the more widely studied community detection problem (Duch and Arenas, 2005; Fortunato, 2010; Newman, 2006); however, there are important conceptual and practical differences between the two. More specifically, community detection is concerned with clustering or partitioning *all* the vertices of a network into communities or clusters; a cluster is, roughly speaking, a group of vertices exhibiting a different connectivity pattern within the cluster as compared to the connectivity between clusters. In contrast, as we alluded to earlier, vertex nomination is only concerned with identifying a small subset of vertices of interest, and furthermore, these vertices of interest might not form a cluster in the usual sense, e.g., their intraconnectivity does not need to be qualitatively different from their connectivity to other "non-interesting" vertices. Due to this reason, vertex nomination is also not the same as local graph clustering (Spielman and Teng, 2013; Yin et al., 2017) as local graph clustering is concerned with clustering the vertices around the neighbourhood of a given seed vertex; the unknown vertices of interest might or might not be included in that neighbourhood.

Before continuing with our exposition we emphasize that, similar to recommender systems for tabular data or community detection in networks, vertex nomination is intrinsically an unsupervised learning problem. It is universally accepted that these type of problems generally do not have clearly defined solutions. For example, given a collection of data points in \mathbb{R}^d , there can be numerous different ways to group these data points into clusters and furthermore all of these clusterings can be valid, and the preference for one clustering over another clustering depends on the setting and/or objective of the data analysis at hand. Analogously, given a graph G , what characterizes a vertex v or a collection of vertices S in G as being interesting is in general not well-defined and could vary between applications and/or between users. Therefore, to present a relevant notion of "interestingness", it is usually assumed that there exists a generative process underlying the observed graph(s); the process itself could be latent or partially observed. This is similar to the use of stochastic blockmodels or its variants in the context of community detection, the use of the Bradley-Terry model in ranking problems, and the assumption of low-rank fac-

tor models in recommender systems. Furthermore, even when we assume that the latent generative model belongs to a collection of models denoted by \mathcal{M} , if \mathcal{M} is not sufficiently restricted then there does not exist a vertex nomination algorithm that is well-behaved for all models in \mathcal{M} , i.e., for any algorithm \mathcal{A} there exists a model $M_0 \in \mathcal{M}$ such that the nomination accuracy of \mathcal{A} when given data generated from M_0 is no better than random guessing; see [Lyzinski et al. \(2019\)](#) for a more precise formulation and statement of this result. In light of the above discussion, in this paper we shall present our methodology in the context of a generative model for which there are latent but unobserved features associated with the vertices and, from these latent features, we can define an appropriate notion of “interestingness”. Similarly, our real data analysis examples are motivated by datasets where there are one-to-one correspondence between (a subset of) the vertices.

Typical applications of vertex nomination include predicting group membership in social networks ([Coppersmith and Priebe, 2012](#)), searching and indexing in databases ([Levin, 2017](#)), and identifying specific type of neurons (e.g., motor neurons) in neuroscience ([Fishkind et al., 2015](#)). A sizable number of techniques have been developed for vertex nomination in the single graph setting, including methods based on likelihood maximization, Bayesian MCMC, and spectral decomposition of the adjacency matrices, see [Coppersmith and Priebe \(2012\)](#); [Fishkind et al. \(2015\)](#); [Lee and Priebe \(2012\)](#); [Lyzinski et al. \(2016\)](#); [Sun et al. \(2012\)](#); [Yoder et al. \(2020\)](#) and the references therein. Among these diverse techniques, the spectral decomposition approach is one of the most practical as it is computationally efficient and can be scaled to handle reasonably large and sparse networks.

The current paper focuses on another important, albeit much less studied, variant of the vertex nomination problem, namely vertex nomination across graphs. More specifically, given two networks G_1 and G_2 and a vertex of interest x in the network G_1 , our task is to find the corresponding vertex of x in G_2 (if it exists). We emphasize that G_1 and G_2 need not have the same number of vertices and that the correspondence between the vertices of G_1 and G_2 is largely unknown. For example, given two social network with some shared people and a particular individual of interest in one network, we wish to identify this individual in another social network, with or without some identity information of other

shared individuals (Patsolic et al., 2017). Further examples include identifying topics of interest across graphical knowledge bases (Sun and Priebe, 2013) and identifying structural signal across connectomes (Sussman et al., 2020).

Two algorithms were recently proposed for this multi-graph vertex nomination problem. The authors of Agterberg et al. (2019) proposed an algorithm based on spectral graph embedding wherein (1) the graphs are spectrally embedded into Euclidean space, (2) the embedded points are aligned via orthogonal Procrustes transformation, (3) the embedded points are simultaneously clustered via Gaussian mixture modeling (Fraley and Raftery, 1998), and (4) output the candidate vertices using the resulting clustering. In contrast, the authors of Patsolic et al. (2017) proposed an algorithm based on seeded graph matching (Lyzinski et al., 2014) wherein they graph match induced subgraphs generated around neighbourhoods of the vertices with known correspondence in each network.

The proposed algorithm in this paper also uses spectral graph embedding. It is noted, empirically, that spectral graph embedding approaches are much faster and more scalable, computationally, as compared to graph matching approaches. Our approach is similar to Agterberg et al. (2019) in that we also spectrally embed the graphs into a common Euclidean space. However, in contrast to the Gaussian mixture modeling of Agterberg et al. (2019), our nomination lists are based on solving a penalized linear assignment problem, and are thus not dependent on tuning parameters such as the number of clusters and the shape/orientation of these clusters, both of which are hard to tune and could have significant impacts on the ordering in the nomination lists. Indeed, if the embedding dimension d is moderately large, a Gaussian mixture model with arbitrary covariance matrices requires estimation of $O(Kd^2)$ parameters where K is the maximum number of Gaussian component.

We also prove consistency results about our scheme when the number of vertices goes to infinity under mild assumptions for a wide class of popular random graph models. Furthermore, for a class of random graph model where the edges of the two graphs are pairwise correlated, we analyze how the magnitude of this correlation influences the consistency.

2 Methodology

We first introduce some notations. Let the two graphs be denoted as $G_1 = (V_1, E_1)$ and $G_2 = (V_2, E_2)$ where V_1 and V_2 are the vertices sets and E_1 and E_2 are the edges sets. We shall assume that our graphs are *undirected*. We also partition the vertices sets V_1 and V_2 as $V_1 = U_1 \cup J_1$ and $V_2 = U_2 \cup J_2$ where U_1 and U_2 denote the sets of *shared* vertices between G_1 and G_2 . We emphasize that the correspondence between the vertices in U_1 and U_2 are only partially known, i.e, we further partition U_1 and U_2 as $U_1 = \{x\} \cup S_1 \cup W_1$ and $U_2 = \{\sigma(x)\} \cup S_2 \cup W_2$ where x denote the *known* vertex of interest in G_1 ; $\sigma : U_1 \rightarrow U_2$ is a bijection such that for any $v \in U_1$, $\sigma(v)$ is its corresponding vertex in U_2 ; S_1 and S_2 are the seed sets with $|S_1| = |S_2| = K$, where we already know the corresponding relationship, i.e., we know the bijection $\sigma|_{S_1} : S_1 \rightarrow S_2$; and W_1 and W_2 are the remaining vertices of interest. We shall assume that the mapping σ from W_1 to W_2 is unknown, and furthermore, recovery of this correspondence between W_1 and W_2 is (often) not of prime concern in our vertex nomination task. In summary, we only know the correspondence between S_1 and S_2 , and given the known vertex of interest x , we are interested in finding its *unknown* correspondence $\sigma(x) \in V \setminus S_2$. Our goal is thus to seek a nomination list of the vertices in $V_2 \setminus S_2$, ranked according to our confidence in how similar they are to x .

We now describe our algorithm for finding $\sigma(x)$. Our algorithm proceeds in three main steps. In the first step we spectrally embed each graph into some d -dimensional Euclidean space. We next aligned these embeddings either via solving an orthogonal Procrustes problem in the case when K , the number of seeds vertices, is at least as large as the embedding dimension d , or via solving a point set registration problem. Finally we solve a quadratic program, using the pairwise distances between the embedded points, to map each vertex $v \in V_1 \setminus S_1$ to some *ordered subset* $\ell(v) \subset V_2 \setminus S_2$; $\ell(v)$ serves as the *nomination list* of the vertices in $V_2 \setminus S_2$ most similar to v . We now describe each of these steps in detail.

2.1 Adjacency Spectral Embedding

We spectrally embed the graphs by truncating their eigenvalue decomposition. More specifically, given an $n \times n$ adjacency matrix \mathbf{A} of a graph and a positive integer d for the embedding dimension, we compute

$$\mathbf{A} = \sum_{i=1}^n \lambda_i u_i u_i^\top,$$

where $|\lambda_1| \geq |\lambda_2| \geq \dots$ are the eigenvalues and u_1, u_2, \dots, u_n are the corresponding eigenvectors. The adjacency spectral embedding of \mathbf{A} (into \mathbb{R}^d) is then the $n \times d$ matrix

$$\hat{\mathbf{X}} = [|\lambda_1|^{1/2} u_1, |\lambda_2|^{1/2} u_2, \dots, |\lambda_d|^{1/2} u_d].$$

The rows of $\hat{\mathbf{X}}$ represent the (low-dimensional) embedding of the vertices of \mathbf{A} into \mathbb{R}^d .

2.2 Orthogonal Procrustes and Point Set Registration

We applied adjacency spectral embedding to the graphs G_1 and G_2 , thereby obtaining the $n \times d$ matrices $\hat{\mathbf{X}}_1$ and $\hat{\mathbf{X}}_2$, respectively. As the rows of $\hat{\mathbf{X}}_1$ and $\hat{\mathbf{X}}_2$ represent the low-dimensional embeddings of the vertices in G_1 and G_2 , we should expect that, for similar vertices, these rows are close in ℓ_2 distance. This is, however, not necessarily the case as the embeddings $\hat{\mathbf{X}}_1$ and $\hat{\mathbf{X}}_2$ are not unique, i.e., $\hat{\mathbf{X}}_1$ and $\hat{\mathbf{X}}_2$ are only defined up to some orthogonal transformations as the eigendecomposition of \mathbf{A}_1 is not, in general, unique. We thus need to align $\hat{\mathbf{X}}_1, \hat{\mathbf{X}}_2$ by an orthogonal transformation \mathbf{W} to eliminate this potential non-identifiability. We describe two methods for finding $\hat{\mathbf{W}}$. The first method is applicable when K , the number of seed vertices, is larger than or equal to d , the embedding dimension; the second method, which is more general but possibly less accurate, is applicable for $K < d$, including the important case of $K = 0$.

2.2.1 Orthogonal Procrustes (when $K \geq d$)

When the number of seed vertices is greater than or equal to the embedding dimension, we find the orthogonal transformation $\hat{\mathbf{W}}$ by solving the orthogonal Procrustes problem

(Schönemann, 1966) to align the seeded vertices across graphs, i.e.,

$$\hat{\mathbf{W}} = \arg \min_{\mathbf{W} \in \mathbb{O}_d} \|(\hat{\mathbf{X}}_1)_{S_1} \mathbf{W} - (\hat{\mathbf{X}}_2)_{S_2}\|_F,$$

where \mathbb{O}_d is the set of all $d \times d$ orthogonal matrices and $(\hat{\mathbf{X}}_1)_{S_1}$ is a $|S_1| \times d$ matrix whose rows are the rows of $\hat{\mathbf{X}}_1$ indexed by the seed set S_1 . With $S_2 = \{\sigma(v) : v \in S_1\}$, $(\hat{\mathbf{X}}_2)_{S_2}$ is defined similarly, so that the i th row of $(\hat{\mathbf{X}}_1)_{S_1}$ corresponds to the i th row of $(\hat{\mathbf{X}}_2)_{S_2}$. The minimizer $\hat{\mathbf{W}}$ has an explicit solution as $\hat{\mathbf{W}} = \mathbf{U}\mathbf{V}^\top$ where $\mathbf{U}\mathbf{D}\mathbf{V}^\top$ is the singular value decomposition of the $d \times d$ matrix $\hat{\mathbf{X}}_2^\top \hat{\mathbf{X}}_1$. After finding $\hat{\mathbf{W}}$ we set $\tilde{\mathbf{X}}_1 = \hat{\mathbf{X}}_1 \hat{\mathbf{W}}$.

2.2.2 Adaptive Rigid Point Set Registration (when $K < d$)

Even when we do not have enough seed vertices or even no seed set ($K = 0$), as long as we have a reasonable number of vertices that are shared between the two graphs, we can apply the coherent point drift algorithm in Myronenko and Song (2010) to align $\hat{\mathbf{X}}_1$ and $\hat{\mathbf{X}}_2$. The algorithm in Myronenko and Song (2010) finds an affine transformation to best align the centroids of the clusters of $\hat{\mathbf{X}}_1$ to the centroids of the clusters of $\hat{\mathbf{X}}_2$. More specifically, given a $n \times d$ matrix $\hat{\mathbf{X}}_1$ and $m \times d$ matrix $\hat{\mathbf{X}}_2$, we find $s \in \mathbb{R}$, $t \in \mathbb{R}^d$ and $\mathbf{W} \in \mathbb{O}_d$ that minimize the following objective function

$$Q(\mathbf{W}, \mathbf{t}, s, \sigma^2) = \frac{1}{2\sigma^2} \sum_{i=1}^n \sum_{j=1}^m P(i | (\hat{\mathbf{X}}_2)_j) \|(\hat{\mathbf{X}}_2)_j - s\mathbf{W}(\hat{\mathbf{X}}_1)_i - \mathbf{t}\|^2 + \frac{N_{\mathbf{P}}d}{2} \log \sigma^2,$$

where $(\hat{\mathbf{X}}_1)_i$ represents the i th row of $\hat{\mathbf{X}}_1$, i.e., the i th vertex's embedding of G_1 ; $(\hat{\mathbf{X}}_2)_j$ is defined similarly. Here $N_{\mathbf{P}} = \sum_{i=1}^n \sum_{j=1}^m P(i | (\hat{\mathbf{X}}_2)_j)$ is a normalizing constant, with $P(i | (\hat{\mathbf{X}}_2)_j)$ the correspondence probability between two vertices' embeddings $(\hat{\mathbf{X}}_1)_i$ and $(\hat{\mathbf{X}}_2)_j$, defined as the posterior probability of the centroid given the vertex's embedding $(\hat{\mathbf{X}}_2)_j$, i.e.,

$$P(i | (\hat{\mathbf{X}}_2)_j) = \frac{\exp\left(-\frac{1}{2}\|((\hat{\mathbf{X}}_2)_j - s\mathbf{W}(\hat{\mathbf{X}}_1)_i - \mathbf{t})/\sigma\|^2\right)}{c + \sum_{k=1}^n \exp\left(-\frac{1}{2}\|((\hat{\mathbf{X}}_2)_j - s\mathbf{W}(\hat{\mathbf{X}}_1)_k - \mathbf{t})/\sigma\|^2\right)},$$

for some constant c (where c is a function of the model parameters defined above; see Myronenko and Song (2010)). The minimization of Q is done via an EM-algorithm. For more details, please refer to Myronenko and Song (2010).

The resulting minimizer $(\hat{s}, \hat{\mathbf{t}}, \hat{\mathbf{W}})$ yield an affine transformation \mathcal{T} of $\hat{\mathbf{X}}_1$ via $\mathcal{T}((\hat{\mathbf{X}}_1)_i) = s\hat{\mathbf{W}}(\hat{\mathbf{X}}_1)_i + \hat{\mathbf{t}}$. We note, however, that in the context of our current work, the alignment of $\hat{\mathbf{X}}_1$ and $\hat{\mathbf{X}}_2$ does not require the scaling s and the translation t . We thus make a few minor adjustments to the EM algorithm in [Myronenko and Song \(2010\)](#). In particular, 1) we always set $s = 1$ and $\mathbf{t} = \mathbf{0}$; 2) we iteratively update \mathbf{W} via $\mathbf{W} = \mathbf{U}\mathbf{V}^T$ instead of $\mathbf{W} = \mathbf{U}\mathbf{C}\mathbf{V}^T$; 3) we initialize \mathbf{W} as a diagonal matrix with 1 or -1 diagonal elements so that the initial error in the EM approach $\sigma^2 = \frac{1}{dnm} \sum_{i=1}^n \sum_{j=1}^m \left\| (\hat{\mathbf{X}}_1 \mathbf{W}^T)_i - (\hat{\mathbf{X}}_2)_j \right\|^2$ is as small as possible. Once we get the final orthogonal matrix $\hat{\mathbf{W}} \in \mathbb{R}^{d \times d}$, we set $\tilde{\mathbf{X}}_1 = \hat{\mathbf{X}}_1 \hat{\mathbf{W}}^T$.

2.3 Quadratic Program

We now formulate a quadratic program to find, for each vertex $v \in V_1$, a collection of vertices $\ell(v) \subset V_2 \setminus S_2$ that are “most similar” to v . Here similarity between $v \in V_1$ and $u \in V_2$ is measured in terms of the Euclidean distances between their embeddings. In other words, given a *query* vertex v in the first graph, our proposed algorithm outputs a nomination list $\ell(v)$ of vertices in the second graph that are most similar to v ; these vertices are deemed “interesting” in the context of the query vertex v .

Our quadratic program is described as follows. Given the aligned embeddings $\tilde{\mathbf{X}}_1$ and $\hat{\mathbf{X}}_2$, we find $\hat{\mathbf{D}}$ to minimize the following objective function

$$\hat{\mathbf{D}} = \arg \min_{\mathbf{D} \in \mathbb{R}^{n \times m}} \sum_{i=1}^n \sum_{j=1}^m \|(\tilde{\mathbf{X}}_1)_i - (\hat{\mathbf{X}}_2)_j\|_2 \cdot \mathbf{D}_{i,j} + \lambda \|\mathbf{D}\|_F^2, \quad (1)$$

subject to the constraints that

- (i.) $\sum_{j=1}^m \mathbf{D}_{i,j} = m$, for all $1 \leq i \leq n$,
- (ii.) $\sum_{i=1}^n \mathbf{D}_{i,j} = n$, for all $1 \leq j \leq m$,
- (iii.) $\mathbf{D}_{i,j} \geq 0$, for all $1 \leq i \leq n, 1 \leq j \leq m$,
- (iv.) $\mathbf{D}_{(S_1)_k, (S_2)_k} = \min\{n, m\}$, for all $1 \leq k \leq K$.

Here $\|(\hat{\mathbf{X}}_1)_i - (\hat{\mathbf{X}}_2)_j\|_2$ is the Euclidean distance between the i th vertex’s embedding of G_1 and the j th vertex’s embedding of G_2 , $\lambda > 0$ is a penalty parameter, and $(S_1)_k, (S_2)_k$

represents the index of the k th seed vertex in G_1 and G_2 , respectively.

The motivation behind solving the above optimization problem is as follows. The constraints on \mathbf{D} state that (1) each vertex $i \in V_1$ is mapped to some collection of vertices in $j \in V_2$, namely those for which $\hat{\mathbf{D}}_{ij} > 0$ (constraint iii.); (2) since for any $i \in V_1$, $\sum_j \hat{\mathbf{D}}_{ij} = m$ where $m = |V_2|$, larger values of $\hat{\mathbf{D}}_{ij}$ indicates more "similarity" between $i \in V_1$ and $j \in V_2$ (constraints i. and ii.); and (3) a seed vertex $s \in S_1$ will get mapped to its unique correspondence $\sigma(s) \in S_2$ (constraint iv.).

We now consider the objective function. The first part of the objective function indicates that the similarity between the i th vertex in V_1 and the j th vertex in V_2 is based on the Euclidean distance $\|(\tilde{\mathbf{X}}_1)_i - (\tilde{\mathbf{X}}_2)_j\|$, i.e., larger distance should lead to smaller $\hat{\mathbf{D}}_{ij}$. We can then consider, for each $i \in V_1$, the nomination list for i as being the vertices in $V_2 \setminus S_2$ arranged according to decreasing values of $\{\hat{\mathbf{D}}_{ij}\}_{j \in V_2 \setminus S_2}$. The second part of the objective function, i.e., the penalty term $\lambda \|\mathbf{D}\|_F^2$, is to discourage sparsity in the rows of $\hat{\mathbf{D}}$. More specifically, removal of the penalty term $\lambda \|\mathbf{D}\|_F^2$ leads to a linear programming problem for which the minimizer $\hat{\mathbf{D}}$ may lie on the boundary of the feasibility region, i.e., the elements of $\hat{\mathbf{D}}$ take values only in $\{0, m, n\}$. If $\hat{\mathbf{D}}_{i,j} = m$, then the i th vertex in V_1 is mapped to the j th vertex in V_2 and if $\hat{\mathbf{D}}_{i,j} = n$ then the j th vertex in V_2 is mapped to the i th vertex in V_1 . This gives a nomination list with a single candidate. This type of nomination list, when accurate, can significantly reduces the burden of post-processing and checking/verifying multiple candidates. However, it is also likely to be non-robust. By adding the penalty term, we encourage the elements in each row of $\hat{\mathbf{D}}$ to be more uniform since, for any vector $x \in \mathbb{R}^m$, $\|x\|_{\ell_2} \geq m^{-1/2} \|x\|_{\ell_1}$ with equality if and only if all the elements of x are the same. We note that the optimization problem in Eq. (1) is analogous to the *quadratically regularized* optimal transport problem between the point masses induced by $\tilde{\mathbf{X}}_1$ and $\tilde{\mathbf{X}}_2$.

The resulting optimization problem is a quadratic program with linear constraints, and the coefficient matrix of the quadratic term is positive definite. Thus, for a fixed $\lambda > 0$, the optimization function is strongly convex and hence there exists a *unique* global minimizer $\hat{\mathbf{D}}$ for any given $\tilde{\mathbf{X}}_1$ and $\tilde{\mathbf{X}}_2$. In particular, for a fixed $\lambda > 0$, the solution $\hat{\mathbf{D}}_\lambda$ of Eq. (1) is

of the form (Blondel et al., 2018)

$$\hat{\mathbf{D}}_\lambda(i, j) = \frac{1}{\lambda} \left[\|(\tilde{\mathbf{X}}_1)_i - (\hat{\mathbf{X}}_2)_j\| - \hat{\alpha}_i - \hat{\beta}_j \right]_+,$$

where $[z]_+ = \max\{z, 0\}$ and $\hat{\boldsymbol{\alpha}} = (\hat{\alpha}_1, \dots, \hat{\alpha}_n)$ and $\hat{\boldsymbol{\beta}} = (\hat{\beta}_1, \dots, \hat{\beta}_m)$ solves the unconstrained dual problem

$$\max_{\boldsymbol{\alpha} \in \mathbb{R}^n, \boldsymbol{\beta} \in \mathbb{R}^m} n\boldsymbol{\alpha}^\top \mathbf{1} + m\boldsymbol{\beta}^\top \mathbf{1} - \frac{1}{2\lambda} \sum_{i=1}^n \sum_{j=1}^m \left[\|(\tilde{\mathbf{X}}_1)_i - (\hat{\mathbf{X}}_2)_j\| - \alpha_i - \beta_j \right]_+.$$

The optimal solution can be found, theoretically, in polynomial time using the ellipsoid algorithm of Kozlov et al. (1980). In practice we use the Gurobi solver (Incorporated, 2015) which is based on an interior-point algorithm. We note that, empirically, the nomination list found by our algorithm is *not* overly sensitive to the choice of the λ , as λ mainly influences the magnitudes of the elements in $\hat{\mathbf{D}}$ but does not changes their relative ordering.

3 Theoretical results

We now investigate the theoretical properties of our proposed algorithm. For simplicity we will only consider the case where G_1 and G_2 have the same number of vertices; the analysis presented here will also extends to the case when G_1 and G_2 have different number of vertices provided that the number of common vertices is sufficiently large. We first formulate a generative model model for generating pairs of random graphs (G_1, G_2) with underlying latent correspondence σ between the vertices V_1 of G_1 and V_2 of G_2 . We then show, for any arbitrary $x \in V_1$ that our algorithm outputs a nomination list $\ell(x)$ composed of relatively few candidate vertices, and that, with high probability, $\sigma(x) \in \ell(x)$. We next investigate the impact of having seeded vertices. In particular, we propose a procedure for re-ranking the nomination lists in the presence of seed vertices. The empirical results in Section 4 indicates that if the number of seed vertices is not too small, then this optional re-ranking step outputs an improved nomination list $\ell(x)$ compared to the nomination list obtained directly from the quadratic program solution.

Our generative model for pairs of random graphs depends on the following notion of the

generalized random dot product graphs (Rubin-Delanchy et al., 2017; Young and Scheinerman, 2007).

Definition 1 (Generalized random dot product graphs). Let $d \geq 1$ be given and let \mathcal{X} be a subset of \mathbb{R}^d such that $x^\top \mathbf{I}_{p,q} y \in [0, 1]$. Here $\mathbf{I}_{p,q}$ is a $d \times d$ diagonal matrix with diagonal entries containing p “+1” and q “-1” for integers $p, q \geq 0$, $p + q = d$. For a given $n \geq 1$, let \mathbf{X} be a $n \times d$ matrix with rows $X_i \in \mathcal{X}$ for $i = 1, 2, \dots, n$. A random graph G is said to be an instance of a generalized random dot product graph with latent positions \mathbf{X} if the adjacency matrix \mathbf{A} of G is a symmetric matrix whose upper triangular entries $\{\mathbf{A}(i, j)\}_{i \leq j}$ are independent Bernoulli random variables with

$$\mathbf{A}(i, j) \sim \text{Bernoulli}(X_i^\top \mathbf{I}_{p,q} X_j).$$

We use $\text{GRDPG}(\mathbf{P})$ to represent such graph, where $\mathbf{P} = \mathbf{X} \mathbf{I}_{p,q} \mathbf{X}^\top$.

Generalized random dot product graphs are a special case of latent position graphs or graphons (Diaconis and Janson, 2008; Hoff et al., 2002; Lovász, 2012). In the general latent position graph model, each vertex v_i is associated with a latent or unobserved vector X_i and, given the collection of latent vectors $\{X_i\}$, the edges are conditionally independent Bernoulli random variables with $\mathbb{P}[v_i \sim v_j] = \kappa(X_i, X_j)$ for some *symmetric* link function κ . Generalized random dot product graphs can be used to model any latent position graphs where the link function κ is finite-dimensional, i.e., κ is such that for any n and for any collection of latent vectors $\{X_i\}_{i=1}^n$, the $n \times n$ matrix \mathbf{P} with $\mathbf{P}_{ij} = \kappa(X_i, X_j)$ has rank at most d for some *arbitrary* but fixed d not depending on n . Indeed, as \mathbf{P} is a symmetric matrix with rank at most d , \mathbf{P} has an eigendecomposition as $\mathbf{P} = \mathbf{U} \mathbf{\Lambda} \mathbf{U}^\top$ and hence, taking $\mathbf{X} = \mathbf{U} |\mathbf{\Lambda}|^{1/2}$ and letting p and q be the number of positive and negative eigenvalues of \mathbf{P} , we obtained a representation of \mathbf{P} as a GRDPG.

Generalized random dot product graphs include, as special cases, the popular class of stochastic blockmodel graphs and their degree-corrected and mixed-membership variants (Airoldi et al., 2008; Holland et al., 1983; Karrer and Newman, 2011).

Definition 2. (Stochastic block model random graphs). We say a random graph G with

adjacency matrix \mathbf{A} is distributed as a stochastic block model random graph with parameters L, b, \mathbf{B} if

1. The vertex set V of G is partitioned into L blocks, $V = V_1 \cup V_2 \cup \dots \cup V_L$.
2. The function b is a mapping from V to $\{1, \dots, L\}$ with $b(i)$ denoting the block label of vertex $i \in V$.
3. The matrix $\mathbf{B} \in [0, 1]^{L \times L}$ is a symmetric matrix of block probabilities. More specifically, given b , the entries $\mathbf{A}_{i,j}$ for $i \leq j$ are *conditionally independent* Bernoulli random variables with $\mathbf{A}_{i,j} \sim \text{Bernoulli}(\mathbf{B}_{b(i),b(j)})$.

We denote a stochastic blockmodel graph as $G \sim \text{SBM}(L, b, \mathbf{B})$.

A L -blocks stochastic blockmodel graph (Holland et al., 1983) corresponds to a GRDPG where \mathcal{X} is a mixture of L point masses. Similarly, a L -blocks degree-corrected stochastic blockmodel and a L -blocks mixed-membership stochastic blockmodel correspond to a GRDPG where \mathcal{X} is supported on a mixture of L rays and on a convex hull of L points, respectively. See Rubin-Delanchy et al. (2017) for a more detailed description of these relationships.

Our generative model for pairs of random graphs extends the GRDPG model for the single graph setting to the setting of two graphs that share a common set of vertices with edges that are possibly correlated.

Definition 3 (ρ -correlated GRDPG). Assume the notation in Definition 1. Let $\rho \in [-1, 1]$ be given. A *pair* of random graphs (G_1, G_2) is said to be an instance of a ρ -correlated generalized random dot product graphs with latent positions \mathbf{X} if the pair of adjacency matrices \mathbf{A}_1 and \mathbf{A}_2 satisfy the following conditions.

1. Marginally $G_1 \sim \text{GRDPG}(\mathbf{P})$ and $G_2 \sim \text{GRDPG}(\mathbf{P})$.
2. Given \mathbf{P} , the bivariate random variables $\{(\mathbf{A}_1)_{i,j}, (\mathbf{A}_2)_{i,j}\}_{1 \leq i < j \leq n}$ are collectively independent and

$$\text{cor}((\mathbf{A}_1)_{i,j}, (\mathbf{A}_2)_{i,j}) = \rho,$$

for any $1 \leq i < j \leq n$.

The correlation ρ in Definition 3 induces a notion of correspondence between the vertices in G_1 and G_2 . More specifically, if $\rho = 0$ then for any two arbitrary pairs of vertices (i, j) and (k, ℓ) , the edges $\mathbf{A}_1(i, j)$ and $\mathbf{A}_2(k, \ell)$ are independent. In contrast, if $\rho \neq 0$ then $\mathbf{A}_1(i, j)$ and $\mathbf{A}_2(k, \ell)$ are independent if and only if $\{i, j\} \neq \{k, \ell\}$. Now suppose that $\rho \neq 0$. Then given a vertex of interest $v \in G_1$, we can define the true correspondence of v in G_2 as the *unique* vertex $\sigma(v) \in G_2$ such that the edges $\mathbf{A}_1(v, u)$ and $\mathbf{A}_2(\sigma(v), \sigma(u))$ are correlated *for all* $u \in G_1$. In summary, if (G_1, G_2) is a pair of ρ -correlated GRDPG graphs with $\rho \neq 0$ then there exists a *canonical* correspondence between the vertices of G_1 and the vertices of G_2 . We use this correspondence to define our notion of “interestingness” when evaluating the proposed methodology on graphs generated from the ρ -GRDPG model, i.e., given a query vertex $v \in G_1$, we wish to find $\sigma(v) \in G_2$. See Agterberg et al. (2019); Lyzinski et al. (2014); Patsolic et al. (2017) for further discussion of the relationship between ρ and its induced correspondence in graph matching and vertex nomination problems.

We now state our first theoretical result. The following result provides an error bound for the $2 \rightarrow \infty$ norm difference between the adjacency spectral embeddings of G_1 and G_2 ; given a $n \times p$ matrix \mathbf{M} with rows \mathbf{M}_i , the $2 \rightarrow \infty$ norm of \mathbf{M} is the maximum ℓ_2 norm of the rows \mathbf{M}_i , i.e.,

$$\|\mathbf{M}\|_{2 \rightarrow \infty} = \max_{\|\mathbf{x}\|_2=1} \|\mathbf{M}\mathbf{x}\|_\infty = \max_{i=1, \dots, n} \|\mathbf{M}_i\|_2.$$

The main feature of the following $2 \rightarrow \infty$ bound is that it is monotone decreasing in both $\rho > 0$ and n , i.e., larger correlation and/or larger number of vertices in each graph lead to smaller error bound that holds *uniformly* for all vertices of G_1 and G_2 . We emphasize that previous bounds for $\min_{\mathbf{W}} \|\hat{\mathbf{X}}_1 \mathbf{W} - \mathbf{X}\|_{2 \rightarrow \infty}$ and $\min_{\mathbf{W}} \|\hat{\mathbf{X}}_2 \mathbf{W} - \mathbf{X}\|_{2 \rightarrow \infty}$ (see e.g., Rubin-Delanchy et al. (2017)) do not depend on the correlation ρ , and thus will lead to a potentially sub-optimal bound of the form

$$\min_{\mathbf{W}} \|\hat{\mathbf{X}}_1 \mathbf{W} - \hat{\mathbf{X}}_2\|_{2 \rightarrow \infty} = O_{\mathbb{P}}(n^{-1/2}).$$

Below, we will characterise the error between asymptotic latent position estimations under the assumption that $\mathbf{P} = \gamma \cdot \mathbf{X} \mathbf{I}_{p,q} \mathbf{X}^\top$ where γ is a sparsity factor.

Theorem 1. *Let $(G_1, G_2) \sim \rho$ -GRDPG(\mathbf{P}), where $\mathbf{P} = \gamma \cdot \mathbf{X} \mathbf{I}_{p,q} \mathbf{X}^\top \in [0, 1]^{n \times n}$ is symmetric with $\text{rank}(\mathbf{P}) = p + q = d$. Suppose that 1) $\max_i \sum_j \mathbf{P}_{i,j}(1 - \mathbf{P}_{i,j}) \geq C \log^4 n$ for some*

universal constant C ; 2) the latent positions satisfy $\frac{1}{n} \sum_{i=1}^n X_i X_i^\top \mathbf{I}_{p,q} \xrightarrow{\text{a.s.}} \Gamma$ as $n \rightarrow \infty$. Here Γ is a fixed $d \times d$ matrix not depending on n . Denote by $\mathbf{A}_1, \mathbf{A}_2 \in \mathbb{R}^{n \times n}$ the adjacency matrices for G_1 and G_2 , respectively. Let $\hat{\mathbf{X}}_1$ and $\hat{\mathbf{X}}_2$ be the adjacency spectral embedding of \mathbf{A}_1 and \mathbf{A}_2 into \mathbb{R}^d , respectively. Then there exists a constant $c > 0$ such that

$$\min_{\mathbf{W} \in \mathbb{O}_d} \left\| \hat{\mathbf{X}}_1 \mathbf{W} - \hat{\mathbf{X}}_2 \right\|_{2 \rightarrow \infty} = (1 - \rho)^{1/2} \cdot O_p(n^{-1/2}) + O_p((\log n)^{2c} n^{-1} \gamma^{-1/2}).$$

Condition (1) in the statement of Theorem 1 is a condition on the *sparsity* of the graph. In particular, Condition (1) is satisfied provided that the *maximum degree* of \mathbf{P} is of order $\Omega(\log^4 n)$. Condition (2) is a condition on the homogeneity of the latent positions \mathbf{X} , i.e., as $n \rightarrow \infty$, the latent positions are sufficiently homogeneous so that their sample second moment matrix $\frac{1}{n} \sum_i X_i X_i^\top \mathbf{I}_{p,q}$ converges. Assuming the above conditions are satisfied, Theorem 1 then implies the existence of an orthogonal \mathbf{W}_* such that for $\rho > 0$ sufficiently bounded away from 1,

$$\|\mathbf{W}_*^\top (\hat{\mathbf{X}}_1)_i - (\hat{\mathbf{X}}_2)_i\| = (1 - \rho)^{1/2} \cdot O_p(n^{-1/2}), \quad \text{for all } i = 1, 2, \dots, n.$$

Suppose we are now given a collection of seed vertices S with $|S| \geq d$, the embedding dimension. Suppose furthermore that the $|S| \times d$ matrices $(\hat{\mathbf{X}}_1)_S$ and $(\hat{\mathbf{X}}_2)_S$ are both of full-column rank, i.e., $(\hat{\mathbf{X}}_1)_S$ and $(\hat{\mathbf{X}}_2)_S$ each contains d linearly independent rows. Then by solving the orthogonal Procrustes problem $\min_{\mathbf{W}} \|(\hat{\mathbf{X}}_1)_S \mathbf{W} - (\hat{\mathbf{X}}_2)_S\|_F$, we will obtain an estimate $\hat{\mathbf{W}}$ of \mathbf{W} that still satisfies the claim in Theorem 1. Indeed, we have

$$\|\hat{\mathbf{W}}^\top (\hat{\mathbf{X}}_1)_j - (\hat{\mathbf{X}}_2)_j\| \leq \|\mathbf{W}_*^\top (\hat{\mathbf{X}}_1)_j - (\hat{\mathbf{X}}_2)_j\| = (1 - \rho)^{1/2} \cdot O_p(n^{-1/2}), \quad \text{for all } j \in S.$$

Now for each $i \notin S$, $(\hat{\mathbf{X}}_1)_i$ and $(\hat{\mathbf{X}}_2)_i$ can be written as a linear combination of $(\hat{\mathbf{X}}_1)_j, j \in S$ and $(\hat{\mathbf{X}}_2)_j, j \in S$, respectively. Hence, by the triangle inequality for vector norms,

$$\|\hat{\mathbf{W}}^\top \hat{\mathbf{X}}_1 - \hat{\mathbf{X}}_2\|_{2 \rightarrow \infty} \leq (1 - \rho)^{1/2} \cdot O_p(n^{-1/2}).$$

In summary, estimates of \mathbf{W}_* using either orthogonal Procrustes or point set registration will yield a transformation $(\tilde{\mathbf{X}}_1)_i$ of $\hat{\mathbf{X}}_1$ whose rows are *uniformly* close to the $(\hat{\mathbf{X}}_2)_i$. Thus, for the optimization problem in Eq. (1), the costs $\hat{c}_{ij} = \|(\tilde{\mathbf{X}}_1)_i - (\hat{\mathbf{X}}_2)_j\|_2$ will be close to that of $c_{ij} = \|(\mathbf{X}_1)_i - (\mathbf{X}_2)_j\|_2$, i.e.,

$$\max_{i \neq j} |\hat{c}_{ij} - c_{ij}| = O_P(n^{-1/2}), \quad \max_i |\hat{c}_{ii} - c_{ii}| = (1 - \rho)^{1/2} O_P(n^{-1/2}).$$

We now consider the implications of Theorem 1 on the solution of the optimization problem in Eq. (1). Suppose first that $\lambda = 0$ so that the optimization problem in Eq.(1) reduces to a linear program. Suppose also that $c_{ij} > 0$ whenever $i \neq j$ and $c_{ii} = 0$, i.e., the latent positions $\{X_i\}$ are unique. Then as $n \rightarrow \infty$, by the above bounds for $|\hat{c}_{ij} - c_{ij}|$, we have $\hat{\mathbf{D}}_{i,i} = n$ for all $1 \leq i \leq n$ and hence, for any vertex of interest x in G_1 , our algorithm will give the nomination list with the true $\sigma(x)$ at the top of the list.

We next consider the case where $\lambda > 0$. Define \mathbf{C} and $\hat{\mathbf{C}}$ as the $n \times n$ matrices whose elements are c_{ij} and \hat{c}_{ij} respectively. Let

$$\mathcal{D} = \{\mathbf{D} : \mathbf{D} \in \mathbb{R}_+^{n \times n}, \mathbf{D}\mathbf{1}_n = (n, \dots, n)^\top, \mathbf{D}^\top \mathbf{1}_n = (n, \dots, n)^\top\}.$$

The optimization problem in Eq. (1) is then equivalent to

$$\operatorname{argmin}_{\mathbf{D} \in \mathcal{D}} \langle \hat{\mathbf{C}}, \mathbf{D} \rangle + \lambda \|\mathbf{D}\|_F^2 = \operatorname{argmin}_{\mathbf{D} \in \mathcal{D}} \|\mathbf{D} + \frac{1}{2\lambda} \mathbf{C}\|_F^2, \quad \lambda > 0.$$

Let $\hat{\mathbf{D}}_\lambda$ be the *unique* solution of the above problem. Then $\hat{\mathbf{D}}_\lambda$ is the *projection* of $-\frac{1}{2\lambda} \hat{\mathbf{C}}$ onto the convex set \mathcal{D} . Now consider the solution of Eq. (1) where we replaced $\hat{\mathbf{C}}$ by \mathbf{C} and denote that unique solution as \mathbf{D}_λ . Then since projection in Frobenius norm onto convex sets is 1-Lipschitz, we have

$$\|\mathbf{D}_\lambda - \hat{\mathbf{D}}_\lambda\|_F \leq \frac{1}{2\lambda} \|\hat{\mathbf{C}} - \mathbf{C}\|_F = \frac{1}{2\lambda} \cdot O_P(n^{1/2}).$$

Since $\|\mathbf{D}\|_F \geq n$ for all $\mathbf{D} \in \mathcal{D}$, we see that $\|\hat{\mathbf{D}}_\lambda - \mathbf{D}_\lambda\|_F = o(\|\mathbf{D}_\lambda\|)$ for all $\lambda \gg n^{-1/2}$. In other words, provided that λ is not too small, the solutions of Eq. (1) using the true cost matrix \mathbf{C} and using the estimated cost matrix $\hat{\mathbf{C}}$ are close, i.e., the relative error between \mathbf{D}_λ and $\hat{\mathbf{D}}_\lambda$ could be made arbitrarily small for sufficiently large n .

Finally, we consider how the solution \mathbf{D}_λ using the true cost matrix \mathbf{C} will look like as $\lambda \rightarrow 0$. Let P_0 be the linear programming problem $\min_{\mathbf{D} \in \mathcal{D}} \langle \mathbf{C}, \mathbf{D} \rangle$. Suppose n is now fixed. Then if $\lambda \rightarrow 0$, \mathbf{D}_λ will converge to the optimal solution with *minimum Frobenius norm* among the set of all optimal solutions of P_0 , i.e., letting ξ_* be the minimum objective value of P_0 , we have

$$\mathbf{D}_\lambda \longrightarrow \operatorname{argmin}_{\mathbf{D} \in \mathcal{D}} \{\|\mathbf{D}\|_F : \langle \mathbf{C}, \mathbf{D} \rangle = \xi_*\}.$$

We note that there could be multiple solutions of $\{\mathbf{D} \in \mathcal{D}: \langle \mathbf{C}, \mathbf{D} \rangle = \xi_*\}$. Nevertheless, in the event that P_0 has a *unique* minimizer, then since $c_{ii} = 0$ for all i , this unique minimizer will be given by $\mathbf{D}_* = \text{diag}(n, n, \dots, n)$. Therefore, by the continuity of the optimization problem, there exists a $\lambda > 0$ such that $\mathbf{D}_\lambda = \mathbf{D}_*$. The previous bound for $\|\hat{\mathbf{D}}_\lambda - \mathbf{D}_\lambda\|_F$ thus suggests that $\hat{\mathbf{D}}_\lambda \rightarrow \mathbf{D}_*$ as $\lambda \rightarrow 0$. A precise statement of this result, however, requires a more detailed analysis of the relationship between λ and n . Indeed, the relative error bound for $\|\hat{\mathbf{D}}_\lambda - \mathbf{D}_\lambda\|_F$ currently requires n sufficiently large and $\lambda \gg n^{-1/2}$ while the convergence of \mathbf{D}_λ to \mathbf{D}_* currently requires $\lambda \rightarrow 0$ with n fixed. We leave this analysis for future work. We summarized the above discussion in the following result.

Proposition 1. *Let P_λ and \hat{P}_λ be the optimization problem in Eq. (1) with cost matrices $\mathbf{C} = (\|(\mathbf{X}_1)_i - (\mathbf{X}_2)_j\|)$ and $\hat{\mathbf{C}} = (\|\hat{\mathbf{W}}(\tilde{\mathbf{X}}_1)_i - (\hat{\mathbf{X}}_2)_j\|)$, respectively. Then for sufficiently large n ,*

$$\frac{\|\mathbf{D}_\lambda - \hat{\mathbf{D}}_\lambda\|_F}{\|\mathbf{D}_\lambda\|_F} = \frac{1}{\lambda} \cdot O(n^{-1/2}).$$

For a fixed n , as $\lambda \rightarrow 0$, we have

$$\mathbf{D}_\lambda \longrightarrow \underset{\mathbf{D} \in \mathcal{D}}{\text{argmin}} \{ \|\mathbf{D}\|_F : \langle \mathbf{C}, \mathbf{D} \rangle = \xi_* \},$$

where ξ_ is the minimum value achieved in P_0 . Furthermore, if $\lambda = 0$ and, for sufficiently large n , P_0 has a unique minimizer $\mathbf{D}_* = \text{diag}(n, n, \dots, n)$, then with high probability $\hat{\mathbf{D}}_0 = \mathbf{D}_*$.*

A special case of Proposition 1 occurs when G_1, G_2 are ρ -correlated stochastic block model graphs. In this setting, the matrix \mathbf{D}_0 will be block-diagonal. Then for sufficiently large n , $\hat{\mathbf{D}}_0$ will also be block-diagonal with high probability. Thus, for ρ -correlated stochastic block models, our algorithm will generally assign each vertex $u \in G_1$ to another vertex $v \in G_2$ from the same block as u . Note that the simulation results in Section 4 are more accurate than what Proposition 1 suggests, i.e., the correlation structure between the two graphs lead to better nomination than just nominating vertices from the same block.

3.1 Reranking Based on Likelihood

The algorithm in Section 2 output a nomination list $\ell(x)$ for the vertex of interest. When the pair (G_1, G_2) is an instance of a ρ -correlated generalized random dot product graph, then for any fixed $\rho > 0$, Theorem 1 guarantees that $\sigma(x)$ is located at the top of the nomination list $\ell(x)$, i.e., $\text{rk}(\sigma(x))/n \rightarrow 0$ as $n \rightarrow \infty$, and furthermore, if $\rho = 1$ then $\text{rk}(\sigma(x)) = 1$ asymptotically almost surely.

We now describe a procedure for refining the nomination list so that $\text{rk}(\sigma(x)) = 1$ even when $\rho < 1$, provided that we have enough seed vertices. Let $v \in V_1$ be given and let $u \in V_2$ be arbitrary. Then for any seed vertex $w \in S_1$ with correspondence $\sigma(w) \in S_2$, we have, by the assumptions on the ρ -correlation structure

$$\begin{aligned}\mathbb{P}(A_1(v, w) = 1, A_2(u, \sigma(w)) = 1) &= P(v, w)^2 + \rho P(v, w)(1 - P(v, w)), \quad u = \sigma(v) \\ \mathbb{P}(A_1(v, w) = 1, A_2(u, \sigma(w)) = 1) &= P(v, w)P(u, \sigma(w)), \quad u \neq \sigma(v)\end{aligned}$$

Let $C_{uvw} = A_1(v, w)A_2(u, \sigma(w)) \in \{0, 1\}$ and let $p_{uvw}(\rho)$ be

$$p_{uvw}(\rho) = P(v, w)P(u, \sigma(w)) + \rho P(v, w)(1 - P(v, w)).$$

Then the collection $\{C_{uvw}\}_{w \in S_1}$ are *independent* Bernoulli random variables with mean parameters $\{p_{uvw}(\rho)\}_{w \in S_1}$ where $\rho > 0$ if and only if $u = \sigma(v)$. For a fixed $\rho > 0$, the likelihood of observing $\{C_{uvw}\}_{w \in S_1}$, assuming the edge probabilities $\{P_{ij}\}_{i < j}$ are known, is then

$$\mathcal{L}(\rho; \{C_{uvw}\}_{w \in S_1}) = \prod_{w \in S_1} (p_{uvw}(\rho))^{c_w} (1 - p_{uvw}(\rho))^{1 - c_w}.$$

Deciding between $u = \sigma(v)$ and $u \neq \sigma(v)$ is thus analogous to testing $\mathbb{H}_0: \rho = 0$ against the $\mathbb{H}_A: \rho \neq 0$. For our problem, the edge probabilities $\{\mathbf{P}_{i,j}\}_{i < j}$ are unknown. Nevertheless, Theorem 1 guarantees that $\{\mathbf{P}_{i,j}\}_{i < j}$ can be estimated uniformly well by $\{\hat{\mathbf{P}}_{i,j}\}_{i < j}$. In summary, our procedure for refining the nomination list $\ell(x)$ is as follows.

- For every v in top ranked part of $\ell(x)$, find $\hat{\rho}_v \in [-1, 1]$ that maximizes the likelihood $\mathcal{L}(\rho; \{C_{xvw}\}_{w \in S_1})$; here the true edge probabilities $\{\mathbf{P}_{i,j}\}$ defining $p_{xvw}(\rho)$ are replaced by their estimates $\{\hat{\mathbf{P}}_{i,j}\}_{i < j}$.
- Reorder these $v \in \ell(x)$ according to decreasing values of $|\rho_v|$.

4 Simulation and Real Data Experiments

We illustrate the performance of our algorithm using two synthetic and real data experiments. For the synthetic data experiments we generate pairs of ρ -correlated GRDPG graphs (G_2, G_2) and, choosing a vertex x at random from G_1 , run our algorithm to find a nomination list $\ell(x) \subset G_2$. For the real data experiments, we use the high-school friendship data from [Moreno and Neville \(2013\)](#) and Microsoft Bing entity graph transitions data from [Agterberg et al. \(2019\)](#). We evaluate the performance of our algorithm using the following two criteria.

- **Mean Reciprocal Rank (MRR)**

The reciprocal rank (RR) of a nomination list $\ell(x)$ is a measure of how far down a ranked list one must go to find the true corresponding vertex of interest $\sigma(x)$, i.e., with a slight abuse of notation,

$$\text{RR}(x) = \text{rk}(\sigma(x))^{-1} \in (0, 1],$$

where $\text{rk}(\sigma(x))$ is the rank of $\sigma(x)$ in $\ell(x)$, with ties broken randomly. For Monte Carlo experiments, we also consider the mean reciprocal rank, i.e., the reciprocal rank averaged over the Monte Carlo replicates; we denote this as MRR. Larger values of RR or MRR indicate better performance.

- **Mean Normalized Rank (MNR)**

The normalized rank (NR) of a nomination list $\ell(x)$ is another measure of the rank of $\sigma(x)$ in $\ell(x)$, and is defined as

$$\text{NR}(x) = \frac{\text{rk}(\sigma(x)) - 1}{|V_2 \setminus S_2| - 1} \in [0, 1],$$

where $|V_2 \setminus S_2|$ is the set of all possible *non-seed* candidates. Note that $\text{NR}(x) = 0$ if and only if $\text{rk}(\sigma(x)) = 1$. For Monte Carlo experiments we also consider the mean normalized rank (MNR). Smaller values of NR or MNR indicate better performance.

4.1 Simulation Experiments

We consider two special cases of the ρ -correlated GRDPG model. The first assumes that the matrix of edge probabilities is positive semidefinite, i.e., that $q = 0$ in the GRDPG model. We refer to this as the ρ -RDPG or ρ -correlated random dot product graphs mode. The second assumes that the edge probabilities matrix is that of the popular stochastic blockmodel graphs [Holland et al. \(1983\)](#).

In the case of ρ -RDPG, we generate pairs of graphs (G_1, G_2) on $n = 300$ vertices where the latent positions $\{\mathbf{X}_i\}$ are sampled uniformly on the unit sphere in \mathbb{R}^3 . We then chose, uniformly at random, a vertex $x \in V_1$ and use our algorithm to find a nomination list $\ell(x) \subset V_2$. Recall that the edges of the graphs are pairwise correlated. This correlation structure then yields a canonical notion of correspondence between the vertices in G_1 and those in G_2 . In other words, given any vertex $v \in G_1$ with latent position X_v , the most “interesting” or “similar” vertex to v in G_2 is simply the vertex $u \in G_2$ with latent position $X_u = X_v$. We evaluate our algorithm using the mean reciprocal rank (MRR) and the mean normalized rank (MNR) calculated from 500 Monte Carlo replicates. The results, as a function of the correlation $\rho \in \{0, 0.3, 0.5, 0.7, 1\}$, are presented in [Figure 1](#). The embeddings of the graphs are aligned either via orthogonal Procrustes (see [Section 2.2](#)) or via the adaptive point set registration procedure of [Myronenko and Song \(2010\)](#).

The setup for ρ -SBM(L, b, \mathbf{B}) is similar. We generate pairs of graphs on $n = 300$ vertices with $L = 3$ blocks and 100 vertices in each block. The block probabilities matrix is

$$\mathbf{B} = \begin{bmatrix} 0.7 & 0.3 & 0.4 \\ 0.3 & 0.7 & 0.2 \\ 0.4 & 0.2 & 0.7 \end{bmatrix}.$$

The mean reciprocal rank (MRR) and the mean normalized rank (MNR), calculated from 500 Monte Carlo replicates, are given in [Figure 2](#).

For these two settings we choose $d = 3$ for the adjacency spectral embedding step, i.e., we embed the graphs into \mathbb{R}^3 . We recall that our algorithm requires alignment of these embeddings either via orthogonal Procrustes or via an adaptive point set registration. These two choices lead to two slightly different quadratic program formulation. More

specifically, as we are embedding into \mathbb{R}^3 , the orthogonal Procrustes procedure needs at least 3 seed vertices to align the embeddings. These seed vertices can then be incorporated into the quadratic program in Section 2.3. In contrast, if the embeddings are aligned using adaptive point set registration, then seed vertices are not necessary and hence the quadratic program is formulated with no seeds. When using orthogonal Procrustes, we also explore the impact of K , the number of seed vertices. We find that increasing K does improve our algorithm, but that the improvement is not overly substantial in the regime where K is small. For example, in the ρ -RDPG setting with $\rho = 0.5$, increasing K from 3 to 9 increases the MRR from 0.29 to 0.39. Thus, for simplicity of presentation, we fixed $K = 6$ for the orthogonal Procrustes step.

The mean reciprocal rank and mean normalized rank of our algorithm, as a function of the correlation coefficient ρ , are presented in Fig. 1 and Fig. 2. Our algorithm is generally quite accurate. In particular, even when $\rho = 0$ our algorithm still performs substantially better than the baseline. We also note that the performance of orthogonal Procrustes (using $K = 6$ seeds) and adaptive point set registration (with no seeds) are similar, with the difference being even less pronounced in the ρ -SBM setting. We posit that the more obvious community structure in the SBM setting helps the adaptive point set registration procedure to align the embeddings more accurately, thereby reducing the need for seed vertices.

We next explore how the reranking step in Section 3.1 can improve the performance of our algorithm, especially when there are enough seed vertices. More specifically, we set $\rho = 0.7$ and vary the number of seed vertices K from 5 to 50. These seed vertices are incorporated into both the quadratic program formulation and the reranking step. We then compare the performance of our algorithm with and without the reranking step. The MRR averaged over 500 Monte Carlo replicates are presented in Fig. 3 for the ρ -RDPG setting and in Fig. 4 for the ρ -SBM setting. These figures indicate that the reranking step leads to significant improvement even for small values of K , e.g., compare the MRR in the ρ -SBM setting with $K = 10$ seeds.

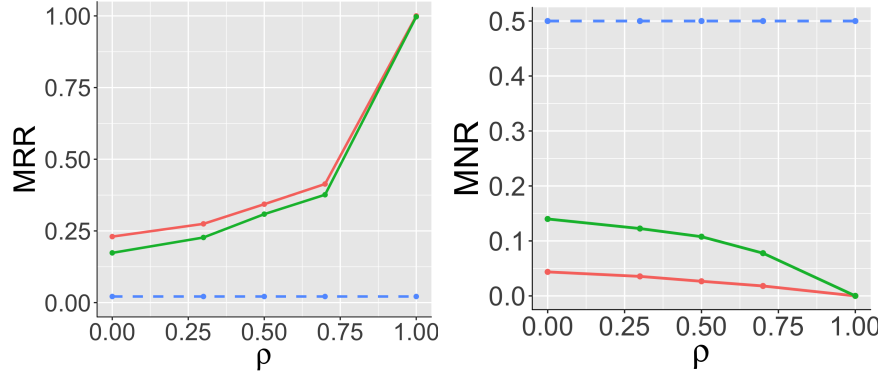


Figure 1: Performance of our algorithm for pairs of ρ -RDPG graphs on $n = 300$ vertices. The mean reciprocal rank (MRR) and mean normalized rank (MNR) are computed based on 500 Monte Carlo replicates. The MRR and MNR are plotted for different values of the correlation coefficient ρ . The red and green lines correspond to the case where the graphs embeddings are aligned via orthogonal Procrustes and via the adaptive point set registration procedure, respectively. The dotted blue lines correspond to the baseline MRR and MNR for a nomination list chosen uniformly at random.

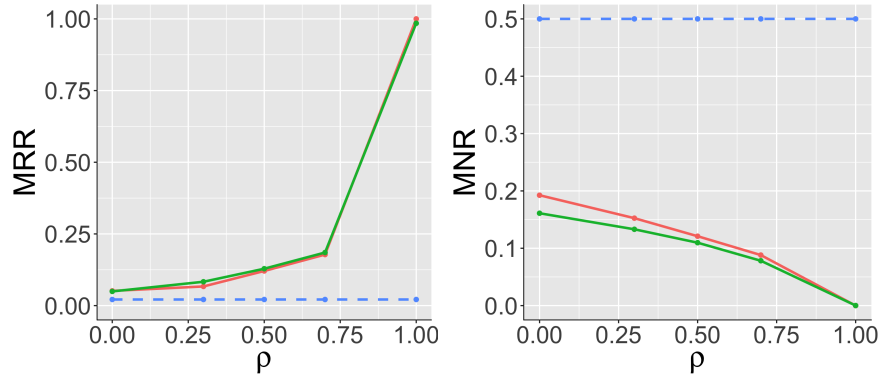


Figure 2: Performance of our algorithm for pairs of ρ -SBM graphs on $n = 300$ vertices. The mean reciprocal rank (MRR) and mean normalized rank (MNR) are computed based on 500 Monte Carlo replicates. See the caption to Figure 1 for further descriptions of the various colored lines.

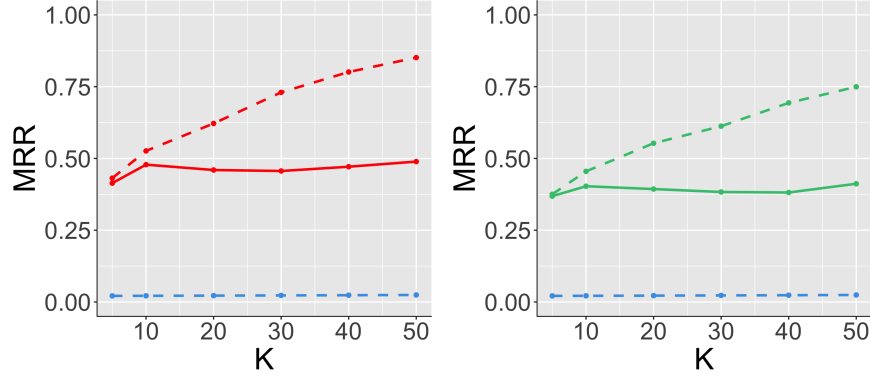


Figure 3: Performance of our algorithm with and without the reranking step for pairs of ρ -RDPG graphs on $n = 300$ vertices. The mean reciprocal rank (MRR) are computed based on 500 Monte Carlo replicates. The red and green lines correspond to the case where the graphs embeddings are aligned via orthogonal Procrustes and via the adaptive point set registration procedure, respectively. In each plot, the corresponding dashed red or green line describes the result after the reranking step. The dotted blue lines correspond to the baseline MRR for a nomination list chosen uniformly at random.

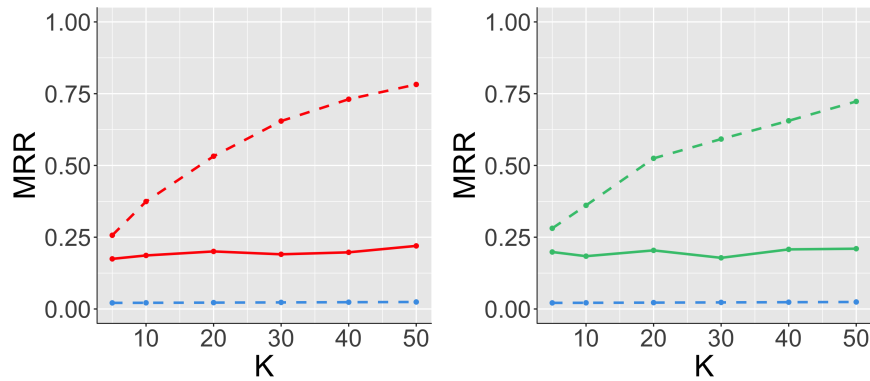


Figure 4: Performance of our algorithm with and without the reranking step for pairs of ρ -SBM(\mathbf{X}) graphs on $n = 300$ vertices. See the caption to Figure 3 for further descriptions.

4.2 Real Data Experiments

We now explore the practical application of our algorithms on real data. In Section 4.2.1, we consider a pair of high-school friendship networks containing some of the same vertices and in which we would like to identify the same individuals across the two networks. Section 4.2.2 explores the graphs derived from Microsoft Bing entity graph transitions.

4.2.1 High School Friendship Networks

We firstly focus on the high school friendship network data from [Mastrandrea et al. \(2015\)](#). This dataset contains two observed graphs and, for each graph, the vertices represent students and the edges represents their friendship. The first graph is extracted from the Facebook social network, i.e., if two individuals were friends on Facebook, then they are adjacent. The second graph is created based on the result of a survey of the students; for every pair of students, they are considered adjacent if at least one of the students in this pair reported that they are friends with the other student. There are 156 vertices in the first graph, 134 vertices in the second graph, and 82 vertices shared between the two graphs. These 82 shared vertices will induce the notion of interestingness for our subsequent analysis. In other words, given a query vertex x in one graph, with x being one of the 82 shared vertices, we are interested in finding the same vertex x in the second graph. This application is thus analogous to that of network deanonymization.

As the number of unshared vertices is reasonably large, we consider two experimental setups. In the first setup we used only the subgraphs induced by the 82 shared vertices while in the other setup we used the full graphs on 156 and 134 vertices. For the adjacency spectral embedding step we set $d = 2$. Orthogonal Procrustes alignment of the embeddings then requires at least 2 seed vertices.

For the experiment using only the shared vertices we iteratively consider each vertex as the vertex of interest. For each vertex of interest we choose a pair of seed vertices, align the embeddings using orthogonal Procrustes, and then solve a quadratic program to obtain a nomination list (the seed vertices are not used in the quadratic program). We repeat this procedure 100 times for each vertex of interest, each time choosing a random pair of seed

vertices. Figure 5 then illustrates, for each of the 82 possible vertex of interest x , how often $\text{NR}(x) \in \{0, (0, 0.2], (0.2, 0.5], (0.5, 1]\}$; the mean normalized rank for a nomination list chosen uniformly at random is 0.5. Figure 5 indicates that the nomination lists obtained by our algorithm are in general quite accurate; indeed, the normalized rank values are small for most of the nomination lists, with a significant portion of the nomination lists even having normalized rank values of 0, i.e., the true correspondence of the vertex of interest is at the top of the nomination list.

We next consider the impact of increasing the number of seed vertices K . For simplicity, we present our analysis for a randomly chosen vertex of interest $x = 27$ as an example. Similar results hold for other vertices. We vary K from 2 to 10 and run 500 Monte Carlo replicates to compute the MNR. We tabulate how often $\text{NR}(x) \in \{0, (0, 0.2], (0.2, 0.5], (0.5, 1]\}$ in Fig. 6. We see from Fig. 6 that $K = 7$ seed vertices is sufficient for the NR of the nomination lists for $x = 27$ to be between 0 and 0.2 always.

Analogous results are available when we align the embeddings using adaptive point set registration procedure. However, since adaptive point set registration does not use any seed vertex, it lead to more robust performance when compared to using orthogonal Procrustes. Finally, we note in passing that our algorithm is quite computationally efficient, e.g., generating Fig. 5 takes us only about 7 minutes on a normal laptop.

We now consider the setup using the full graphs on 134 and 156 vertices. Once again we use orthogonal Procrustes to align the embeddings. We then consider each of the 82 shared vertices as the vertex of interests x and find the nomination list $\ell(x)$ using the same procedure as that outlined above for the setup using the induced subgraphs. Note that the main difference between the current setup and that of the induced subgraphs is that, for each vertex of interest, there are more candidate vertices in the current setup; this make the task harder and hence the performance of our algorithm is likely to be worse in the current setup. The experiment results in Fig. 7 confirmed this speculation. Indeed, comparing Figure 5 and Figure 7, we see that the number of times in which the obtained nomination list is no better than chance increases. Nevertheless, our algorithm is still quite accurate since, for almost all of the vertex of interests, the true correspondences do appear

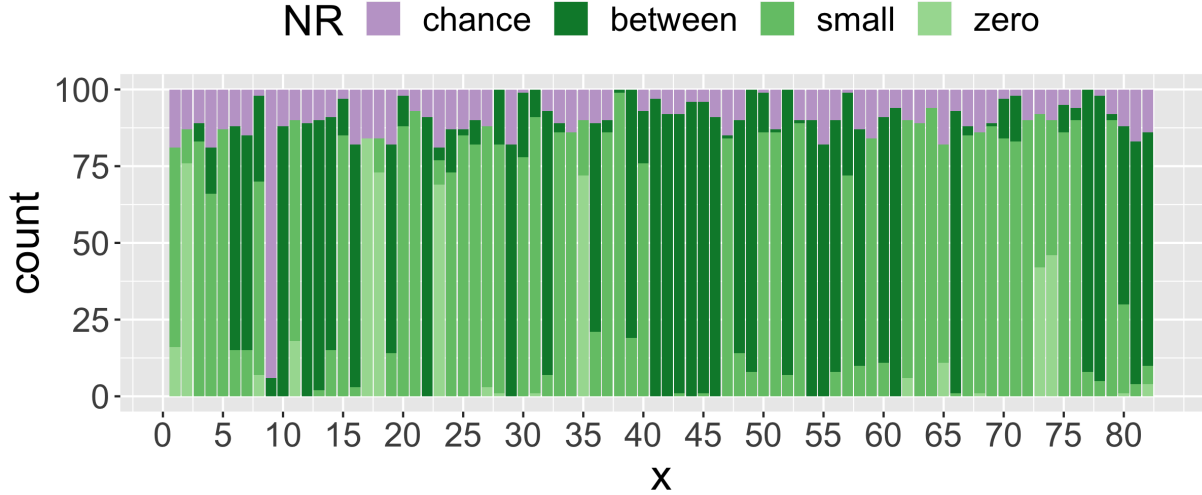


Figure 5: Performance of our algorithm for vertex nomination between the two high-school networks. Here we consider only the subgraphs induced by the 82 shared vertices. The graphs embeddings are aligned via orthogonal Procrustes transformation using two randomly selected seeds; these seeds are only used for the alignment and are not incorporated into the quadratic programming step. For each $x \in V_1$ we repeat this random seed selection 100 times and record the normalized rank of its correspondence $\sigma(x) \in V_2$. The four categories correspond to the case when the normalized rank (NR) is equal to 0, lying between 0 and 0.2, lying between 0.2 and 0.5, or larger than 0.5.

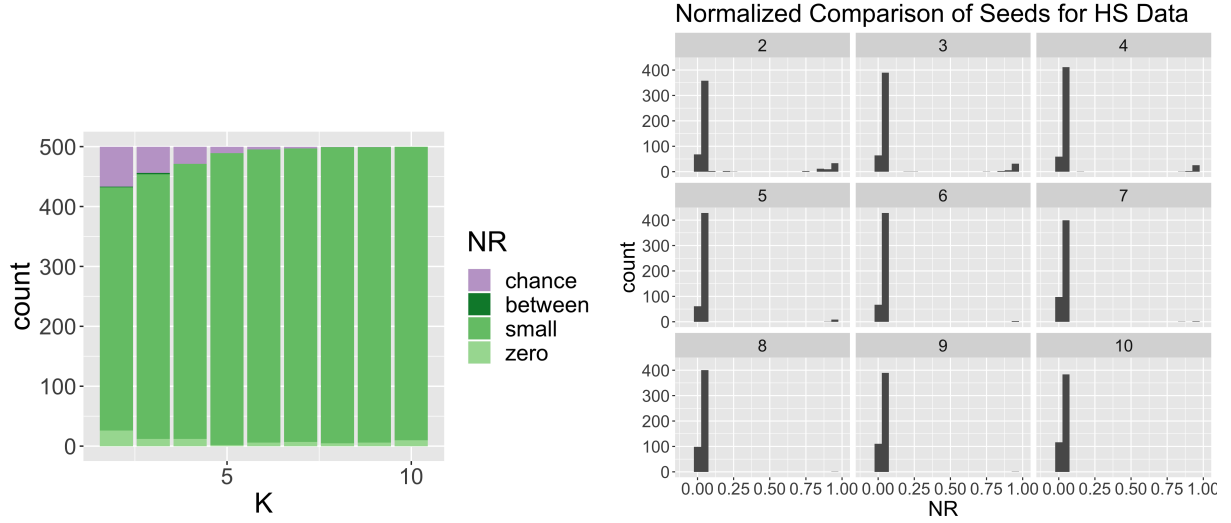


Figure 6: For applying the algorithm with orthogonal Procrustes to subgraphs of high school network generated by shared vertices, using $x = 27$ as the vertex of interest, we vary the number of seed vertices K from 2 to 10, uniformly at random generate 500 sets of seed vertices and plot NR.

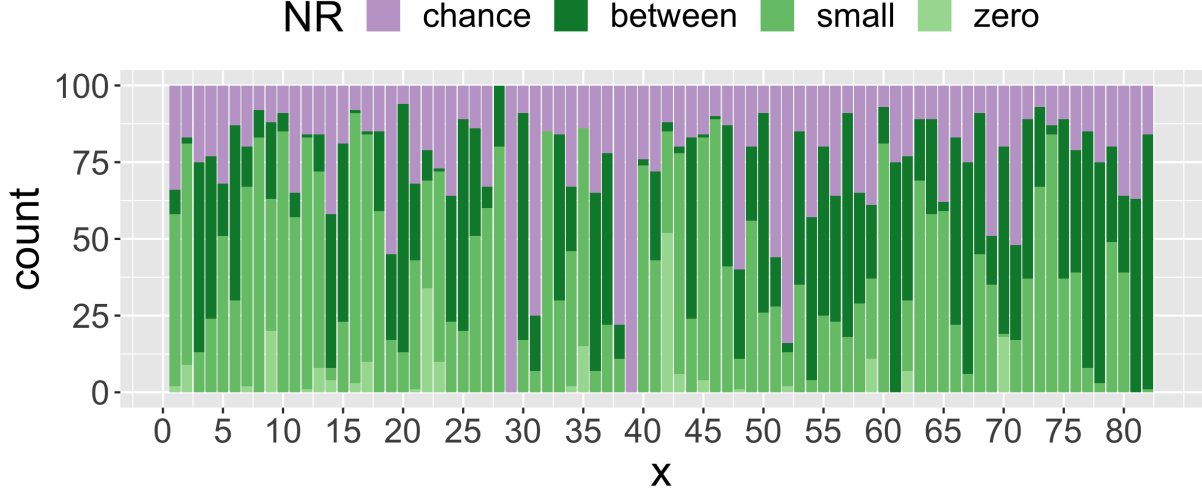


Figure 7: Performance of our algorithm for vertex nomination between the two high-school networks. Here we consider the graphs with full vertices. The graphs embeddings are aligned via orthogonal Procrustes transformation using two randomly selected seeds; these seeds are only used for the alignment and are not incorporated into the quadratic programming step. See the caption to Figure 5 for further descriptions of the experiment.

frequently at the top of the nomination lists.

4.2.2 Microsoft Bing Entity Graph Transitions

In this section, we consider graphs derived from one month of Bing entity graph transitions. The dataset for this example is from [Agterberg et al. \(2019\)](#) and contains two graphs on the *same* set of vertices; these vertices denote entities. The (weighted) edges in each graph represent transition rates between the entities during an internet browsing session, but the types of transitions differ between the two graphs. More specifically, the edges in the first graph G_1 represents transitions that were made using a suggestion interface while the transitions in the second graph G_2 were made independently of any suggestion interface. As the suggestion interface can only suggest a few entities at a time, the edges in G_1 are much more constrained than those in G_2 . The first and second graphs both have 13535 vertices and approximately 5.2×10^5 and 5.9×10^5 edges, respectively. There is, once again, a one-to-one correspondence between the vertices in both networks and we use this correspondence to define our notion of interestingness, i.e., given a vertex x in one graph, we are interested in finding the same vertex in the other graph.

For our first analysis we sub-sample the graphs and only consider the subgraphs induced by the first 1000 vertices. These induced subgraphs are also unweighted, i.e., two vertices are adjacent in a induced subgraph if the corresponding transition rate in the original graph is non-zero. Denoting by G_1 and G_2 the resulting induced subgraphs, G_1 and G_2 have 8365 edges and 10247 edges, respectively. We emphasize that there is a 1-to-1 correspondence between the vertex sets of G_1 and G_2 .

We now explore the performance of our algorithm for vertex nomination between G_1 and G_2 . In particular, we sequentially consider each vertex $x \in G_1$ as the vertex of interest, and for a given vertex of interest we randomly select 10 other vertices as seeds. After computing the NR for all vertices, we present the histogram of NR to show the distribution. The results are given in Figure 8 for both the cases where the graph embeddings are aligned via orthogonal Procrustes and via adaptive point set registration. We emphasize that there are two variants of adaptive point set registration used here. In the first variant the 10 seed

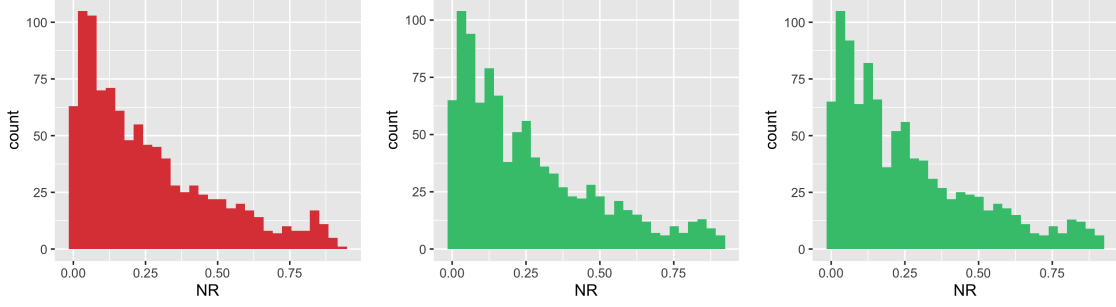


Figure 8: Performance of our algorithm for vertex nomination between the two Microsoft Bing entities transition networks on $n = 1000$ vertices. For each $x \in V_1$ we randomly selected 10 seeds and record the normalized rank (NR) of its correspondence $\sigma(x) \in V_2$. The red and green histogram of NR correspond to the case where the graphs embeddings are aligned via orthogonal Procrustes and via the adaptive point set registration procedure, respectively. The last green figure corresponds to the case for adaptive point set registration procedure without any seeds.

vertices are used in the quadratic programming formulation while in the second variant the seed vertices are not used at all. Fig. 8 indicates that the normalized rank values are generally quite small and hence the nomination lists returned by our algorithm are accurate. Figure 8 also indicates that there is almost no difference between using orthogonal Procrustes and using adaptive point set registration and, more importantly, our algorithm perform well even when there are no seeds information, i.e., the performance of adaptive point set registration with no seeds is virtually identical to that of orthogonal Procrustes and point set registrations with 10 seeds. Indeed, Table 1 summarized the quantiles of the NR for different variants of our algorithm and we see from these quantiles that the performance of the three variants are virtually indistinguishable. For our second analysis we do not sub-sample the graphs and hence G_1 contains 13535 vertices and 519389 edges while G_2 contains the same 13535 vertices and 595047 edges. Once again we sequentially consider each vertex $x \in G_1$ is as the vertex of interest. For a given vertex of interest we randomly select 10 other vertices as seeds. We then take the induced subgraph in G_1 (respectively G_2) formed by the 1-neighborhood of these 11 vertices (the vertex of interest

	1%	5%	10%	25%	50%	75%	95%	99%
Procrustes (10 seeds)	0.003	0.013	0.030	0.074	0.196	0.387	0.750	0.870
set registration (10 seeds)	0.002	0.012	0.025	0.073	0.196	0.387	0.757	0.877
set registration (no seeds)	0.002	0.013	0.025	0.073	0.196	0.386	0.757	0.876

Table 1: Quantile levels and NR values for vertex nomination with the Bing entity networks on $n = 1000$ vertices

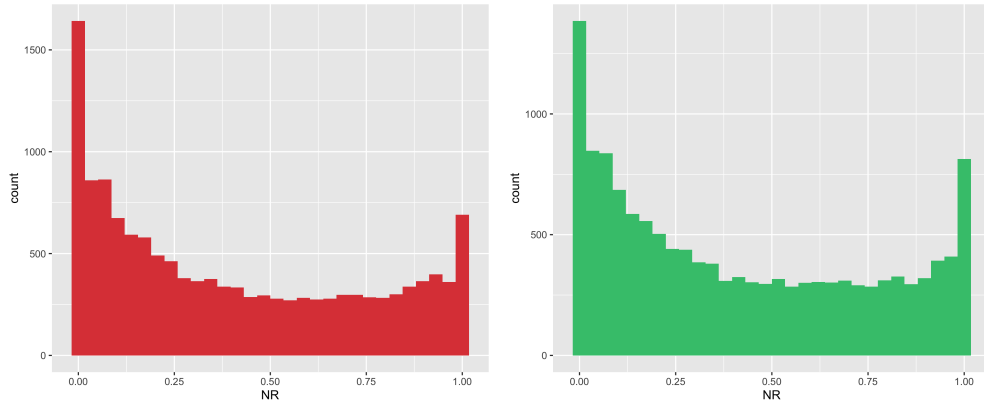


Figure 9: Performance of our algorithm for vertex nomination between the two Microsoft Bing entities transition networks on $n = 13535$ vertices. For each $x \in V_1$ we randomly selected 10 seeds and our algorithms are applied on the 1-neighborhood of them. We record the normalized rank (NR) of its correspondence $\sigma(x)$ in the whole nomination list. The red and green histogram of NR correspond to the case where the graphs embeddings are aligned via orthogonal Procrustes and via the adaptive point set registration procedure, respectively.

and the 10 seed vertices). Letting $G_1(v)$ and $G_2(v)$ denote the induced subgraph of G_1 and G_2 , we then apply our algorithm to find the nomination correspondence $\sigma(x) \in G_2(v)$ for the given vertex of interest $x \in G_1(v)$. The histogram of the NR are summarized in Fig. 9. Figure 9 indicates that, even though there is no longer an exact 1-to-1 correspondence between the vertices set in the induced 1-neighborhood subgraphs, our algorithms still give accurate nomination lists.

	1%	5%	10%	25%	50%	75%	95%	99%
Procrustes (10 seeds)	0.000	0.000	0.007	0.087	0.315	0.699	0.984	1.000
set registration (10 seeds)	0.000	0.000	0.016	0.100	0.338	0.715	0.994	1.000

Table 2: Quantile levels and NR values for vertex nomination with the Bing entity networks on $n = 13535$ vertices

5 Conclusion

In summary, the current paper provides an algorithm for solving the vertex nomination problem in the multi-graphs setting. Our algorithm depends on adjacency spectral embedding and followed by solving a quadratic programming. To eliminate non-identifiability of spectral embedding for different graphs, besides an approach based on orthogonal Procrustes, we propose a method using adaptive point set registration to align the embedding that also work without needing any information about seed vertices. Under mild assumption, we establish theoretical guarantee on the consistency of our nomination scheme. The empirical results on the simulation and real data analysis demonstrate that our algorithm is generally quite accurate even when there are only a few seeds or even no seed vertices. As we allude to in the introduction of this paper, vertex nomination is an unsupervised learning problem and thus evaluation of a vertex nomination algorithm usually requires some underlying ground truth. The real data analysis examples of this paper are based on pairs of graphs with shared vertices and we used these shared vertices to define our groundtruth; the resulting analysis is thus similar to network deanonymization. When there is no known groundtruth, then our proposed methodology can be used for exploratory data analysis or

for suggesting possible matches between a query vertex x in one graph and vertices most “similar” to x in the second graph. To evaluate the accuracy of the resulting nominations will, however, require additional domain knowledge or domain experts. We believe that our chosen examples are simple to describe and yet sufficiently rich in scope, thereby providing a clear and compelling illustration of the effectiveness of our proposed methodology.

While the proposed algorithm is reasonably computationally efficient, there are still technical challenges in applying the algorithm to large graphs. For example the Bing graphs analyzed in this paper are on the order of 10^4 vertices and 10^5 to 10^6 edges and our algorithm takes roughly 30 minutes for one full analysis when ran on a consumer laptop. For larger-scale graphs, such as those on 10^5 vertices and 10^7 edges, our algorithm breaks down. In particular, the EM steps in the adaptive point set registration algorithm can be quite slow to converge and thus might require sub-sampling of the embedded points before performing the alignment. Furthermore, the quadratic programming step requires keeping track of the assignment matrix \mathbf{D} ; a naive approach of storing \mathbf{D} will require too much memory, especially since \mathbf{D} is likely to be sparse throughout the optimization. Development of iterative procedures for storing and updating \mathbf{D} is thus essential for scaling our algorithm to large graphs. We leave these investigations for future work.

References

- Agterberg, J., Y. Park, J. Larson, C. White, C. E. Priebe, and V. Lyzinski (2019). Vertex nomination, consistent estimation, and adversarial modification. arXiv preprint at <http://arxiv.org/abs/1905.01776>.
- Airoldi, E. M., D. M. Blei, S. E. Fienberg, and E. P. Xing (2008). Mixed membership stochastic blockmodels. *Journal of Machine Learning Research* 9, 1981–2014.
- Blondel, M., V. Seguy, and A. Rolet (2018). Smooth and sparse optimal transport. In *Proceedings of the 21st International Conference on Artificial Intelligence and Statistics*, pp. 880–889.

- Cai, T. T. and A. Zhang (2018). Rate-optimal perturbation bounds for singular subspaces with applications to high-dimensional statistics. *The Annals of Statistics* 46, 60–89.
- Coppersmith, G. A. and C. E. Priebe (2012). Vertex nomination via content and context. arXiv preprint at <http://arxiv.org/abs/1201.4118>.
- Diaconis, P. and S. Janson (2008). Graph limits and exchangeable random graphs. *Rendiconti di Matematica, Serie VII* 28, 33–61.
- Duch, J. and A. Arenas (2005). Community detection in complex networks using extremal optimization. *Physical Review E* 72, 027104.
- Fishkind, D. E., V. Lyzinski, H. Pao, L. Chen, and C. E. Priebe (2015). Vertex nomination schemes for membership prediction. *Annals of Applied Statistics* 9, 1510–1532.
- Fortunato, S. (2010). Community detection in graphs. *Physics Reports* 486, 75–174.
- Fraley, C. and A. E. Raftery (1998). Mclust: Software for model-based cluster and discriminant analysis. Technical Report 342, Department of Statistics, University of Washington: Technical Report.
- Hoff, P. D., A. E. Raftery, and M. S. Handcock (2002). Latent space approaches to social network analysis. *Journal of the American Statistical Association* 97(460), 1090–1098.
- Holland, P. W., K. B. Laskey, and S. Leinhardt (1983). Stochastic blockmodels: first steps. *Social Networks* 5(2), 109–137.
- Incorporated, G. O. (2015). Gurobi optimizer reference manual. Available at <http://www.gurobi.com>.
- Karrer, B. and M. E. J. Newman (2011). Stochastic blockmodels and community structure in networks. *Physical Review E* 83(1), 016107.
- Kozlov, M. K., S. P. Tarasov, and L. G. Khachiyan (1980). The polynomial solvability of convex quadratic programming. *USSR Computational Mathematics and Mathematical Physics* 20, 223–228.

- Kudo, T., E. Maeda, and Y. Matsumoto (2005). An application of boosting to graph classification. In *Advances in Neural Information Processing Systems*, pp. 729–736.
- Lee, D. S. and C. E. Priebe (2012). Bayesian vertex nomination. arXiv preprint at <http://arxiv.org/abs/1205.5082>.
- Levin, K. (2017). *Graph Inference with Applications to Low-Resource Audio Search and Indexing*. Ph. D. thesis, Johns Hopkins University.
- Lloyd, J., P. Orbanz, Z. Ghahramani, and D. M. Roy (2012). Random function priors for exchangeable arrays with applications to graphs and relational data. In *Advances in Neural Information Processing Systems*, pp. 998–1006.
- Lovász, L. (2012). *Large networks and graph limits*. American Mathematical Society.
- Lu, L. and X. Peng (2013). Spectra of edge-independent random graphs. *The Electronic Journal of Combinatorics* 20(4), P27.
- Lyzinski, V., D. E. Fishkind, and C. E. Priebe (2014). Seeded graph matching for correlated erdős-rényi graphs. *Journal of Machine Learning Research* 15, 3513–3540.
- Lyzinski, V., K. Levin, D. E. Fishkind, and C. E. Priebe (2016). On the consistency of the likelihood maximization vertex nomination scheme: Bridging the gap between maximum likelihood estimation and graph matching. *Journal of Machine Learning Research* 17, 1–34.
- Lyzinski, V., K. Levin, and C. E. Priebe (2019). On consistent vertex nomination schemes. *Journal of Machine Learning Research* 20, 1–39.
- Mastrandrea, R., J. Fournet, and A. Barrat (2015). Contact patterns in a high school: a comparison between data collected using wearable sensors, contact diaries and friendship surveys. *PLOS One* 10, e0136497.
- Moreno, S. and J. Neville (2013). Network hypothesis testing using mixed kronecker product graph models. In *IEEE 13th International Conference on Data Mining*, pp. 1163–1168.

- Myronenko, A. and X. Song (2010). Point set registration: Coherent point drift. *IEEE Transactions on Pattern Analysis and Machine Intelligence* 32, 2262–2275.
- Newman, M. E. J. (2006). Finding community structure in networks using the eigenvectors of matrices. *Physical Review E* 74, 036104.
- Patsolic, H. G., Y. Park, V. Lyzinski, and C. E. Priebe (2017). Vertex nomination via seeded graph matching. arXiv preprint at <http://arxiv.org/abs/1705.00674>.
- Peyré, G. and M. Cuturi (2019). Computational optimal transport. *Foundations and Trends® in Machine Learning* 11(5-6), 355–607.
- Rubin-Delanchy, P., J. Cape, M. Tang, and C. E. Priebe (2017). A statistical interpretation of spectral embedding: the generalised random dot product graph. arXiv preprint at <http://arxiv.org/abs/1709.05506>.
- Rubin-Delanchy, P., C. E. Priebe, M. Tang, and J. Cape (2017). A statistical interpretation of spectral embedding: the generalised random dot product graph. arXiv preprint at <http://arxiv.org/abs/1709.05506>.
- Schaeffer, S. E. (2007). Graph clustering. *Computer Science Review* 1, 27–64.
- Schönemann, P. H. (1966). A generalized solution of the orthogonal procrustes problem. *Psychometrika* 31, 1–10.
- Spielman, D. A. and S.-H. Teng (2013). A local clustering algorithm for massive graphs and its application to nearly linear time graph partitioning. *SIAM Journal on Computing* 42, 1–26.
- Sun, M. and C. E. Priebe (2013). Efficiency investigation of manifold matching for text document classification. *Pattern Recognition Letters* 34, 1263–1269.
- Sun, M., M. Tang, and C. E. Priebe (2012). A comparison of graph embedding methods for vertex nomination. In *11th International Conference on Machine Learning and Applications*, pp. 398–403.

- Sussman, D., Y. Park, C. E. Priebe, and V. Lyzinski (2020). Matched filters for noisy induced subgraph detection. *IEEE Transactions on Pattern Analysis and Machine Intelligence* 42, 2887–2900.
- Tang, M., A. Athreya, D. L. Sussman, V. Lyzinski, and C. E. Priebe (2017). A semiparametric two-sample hypothesis testing problem for random dot product graphs. *Journal of Computational and Graphical Statistics* 26, 344–354.
- Xu, J. (2017). Rates of convergence of spectral methods for graphon estimation. arXiv preprint at <http://arxiv.org/abs/1709.03183>.
- Yin, H., A. R. Benson, J. Leskovec, and D. F. Gleich (2017). Local higher-order graph clustering. In *Proceedings of the 23rd ACM SIGKDD International Conference on Knowledge Discovery and Data Mining*, pp. 555–564.
- Yoder, J., L. Chen, H. Pao, E. Bridgeford, K. Levin, D. E. Fishkind, C. Priebe, and V. Lyzinski (2020). Vertex nomination: The canonical sampling and the extended spectral nomination schemes. *Computational Statistics & Data Analysis* 145, 106916.
- Young, S. J. and E. R. Scheinerman (2007). Random dot product graph models for social networks. In *International Workshop on Algorithms and Models for the Web-Graph*, pp. 138–149. Springer.
- Yu, Y., T. Wang, and R. J. Samworth (2014). A useful variant of the Davis–Kahan theorem for statisticians. *Biometrika* 102, 315–323.
- Zhang, M., Z. Cui, M. Neumann, and Y. Chen (2018). An end-to-end deep learning architecture for graph classification. In *32nd AAAI Conference on Artificial Intelligence*, pp. 4438–4445.

Proof of Proposition 1

The first part of Proposition 1 has been proved in Section 3. Now we prove the second part, i.e., we will show that for a fixed n , as $\lambda \rightarrow 0$, we have

$$\mathbf{D}_\lambda \longrightarrow \operatorname{argmin}_{\mathbf{D} \in \mathcal{D}} \{\|\mathbf{D}\|_F : \langle \mathbf{C}, \mathbf{D} \rangle = \xi_*\},$$

where ξ_* is the minimum value achieved in P_0 .

The following argument is adapted from the proof of Proposition 4.1 in [Peyré and Cuturi \(2019\)](#). We consider a sequence $(\lambda_\ell)_\ell$ such that $\lambda_\ell \rightarrow 0$ and $\lambda_\ell > 0$. Since \mathcal{D} is bounded, we can extract a sequence (that we do not relabel for the sake of simplicity) such that $\mathbf{D}_{\lambda_\ell} \rightarrow \mathbf{D}^*$. Since \mathcal{D} is closed, $\mathbf{D}^* \in \mathcal{D}$. We consider any \mathbf{D} such that $\langle \mathbf{C}, \mathbf{D} \rangle = \xi_*$, where ξ_* is the minimum value achieved in P_0 . By optimality of such \mathbf{D} and $\mathbf{D}_{\lambda_\ell}$ for their respective optimization problems, we have

$$0 \leq \langle \mathbf{C}, \mathbf{D}_{\lambda_\ell} \rangle - \langle \mathbf{C}, \mathbf{D} \rangle \leq \lambda_\ell \cdot (\|\mathbf{D}\|_F - \|\mathbf{D}_{\lambda_\ell}\|_F). \quad (2)$$

Since $\|\cdot\|_F$ is continuous, taking the limit $\ell \rightarrow +\infty$ in this expression shows that $\langle \mathbf{C}, \mathbf{D}^* \rangle = \langle \mathbf{C}, \mathbf{D} \rangle$ so that \mathbf{D}^* is a feasible point of $\{\mathbf{D} : \langle \mathbf{C}, \mathbf{D} \rangle = \xi_*\}$. Furthermore, dividing by λ_ℓ in Eq. (2) and taking the limit shows that $\|\mathbf{D}^*\|_F \leq \|\mathbf{D}\|_F$, which shows that \mathbf{D}^* is a solution of $\operatorname{argmin}_{\mathbf{D} \in \mathcal{D}} \{\|\mathbf{D}\|_F : \langle \mathbf{C}, \mathbf{D} \rangle = \xi_*\}$.

Proof of Theorem 1

The following argument is adapted from the proof of Theorem 5 in [Rubin-Delanchy et al. \(2017\)](#) for bounding $\|\hat{\mathbf{X}} - \mathbf{X}\|_{2 \rightarrow \infty}$ in the case of a *single* generalized random dot product graph to the current setting of bounding $\|\hat{\mathbf{X}}_1 - \hat{\mathbf{X}}_2\|_{2 \rightarrow \infty}$ for a *pair* of *correlated* generalized random dot product graphs.

We set the block spectral decomposition of the symmetric matrix \mathbf{A}_1 is $\mathbf{A}_1 = [\mathbf{U}_1 | \mathbf{U}'_1][\mathbf{S}_1 \oplus \mathbf{S}'_1][\mathbf{U}_1 | \mathbf{U}'_1]^\top = \mathbf{U}_1 \mathbf{S}_1 \mathbf{U}_1^\top + \mathbf{U}'_1 \mathbf{S}'_1 \mathbf{U}'_1{}^\top$, where the diagonal matrix $\mathbf{S}_1 \in \mathbb{R}^{d \times d}$ contains the d largest-in-magnitude nonzero eigenvalues of \mathbf{A}_1 . Similarly, $\mathbf{A}_2 = \mathbf{U}_2 \mathbf{S}_2 \mathbf{U}_2^\top + \mathbf{U}'_2 \mathbf{S}'_2 \mathbf{U}'_2{}^\top$. According to the definition of adjacency spectral embedding, we know $\hat{\mathbf{X}}_1 = \mathbf{U}_1 |\mathbf{S}_1|^{\frac{1}{2}}$ and

$\hat{\mathbf{X}}_2 = \mathbf{U}_2|\mathbf{S}_2|^{\frac{1}{2}}$. So our goal is to prove

$$\min_{\mathbf{W} \in \mathbb{O}_d} \left\| \mathbf{U}_1|\mathbf{S}_1|^{\frac{1}{2}}\mathbf{W} - \mathbf{U}_2|\mathbf{S}_2|^{\frac{1}{2}} \right\|_{2 \rightarrow \infty} = (1 - \rho)^{1/2} \cdot O_p(n^{-1/2}) + O_p((\log n)^{2c} n^{-1} \gamma^{-1/2}).$$

We set $\mathbf{W}^* = \mathbf{W}_1^\top \mathbf{W}_2$, where $\mathbf{W}_1, \mathbf{W}_2$ are two orthogonal matrices and we will give their specific formula in the following proof. Let $\mathbf{P} = \mathbf{U}\mathbf{S}\mathbf{U}^\top$ be the eigendecomposition of \mathbf{P} where $\mathbf{U} \in \mathbb{R}^{n \times d}$ is the matrix whose columns are the eigenvectors and the diagonal matrix $\mathbf{S} \in \mathbb{R}^{d \times d}$ contains all the d nonzero eigenvalues of \mathbf{P} . Now we split $\mathbf{U}_1|\mathbf{S}_1|^{\frac{1}{2}}\mathbf{W}^* - \mathbf{U}_2|\mathbf{S}_2|^{\frac{1}{2}}$ as

$$\begin{aligned} \mathbf{U}_1|\mathbf{S}_1|^{\frac{1}{2}}\mathbf{W}^* - \mathbf{U}_2|\mathbf{S}_2|^{\frac{1}{2}} &= \underbrace{\left[\mathbf{U}_1|\mathbf{S}_1|^{\frac{1}{2}}\mathbf{W}_1^\top \mathbf{W}_2 - \mathbf{U}\mathbf{U}^\top \mathbf{U}_1|\mathbf{S}_1|^{\frac{1}{2}}\mathbf{W}_1^\top \mathbf{W}_2 \right]}_{\mathbf{T}_1} \\ &\quad + \underbrace{\left[\mathbf{U}\mathbf{U}^\top \mathbf{U}_1|\mathbf{S}_1|^{\frac{1}{2}}\mathbf{W}_1^\top \mathbf{W}_2 - \mathbf{U}|\mathbf{S}|^{\frac{1}{2}}\mathbf{U}^\top \mathbf{U}_1\mathbf{W}_1^\top \mathbf{W}_2 \right]}_{\mathbf{T}_2} \\ &\quad + \underbrace{\left[\mathbf{U}|\mathbf{S}|^{\frac{1}{2}}\mathbf{U}^\top \mathbf{U}_1\mathbf{W}_1^\top \mathbf{W}_2 - \mathbf{U}|\mathbf{S}|^{\frac{1}{2}}\mathbf{W}_1\mathbf{W}_1^\top \mathbf{W}_2 \right]}_{\mathbf{T}_3} \\ &\quad + \underbrace{\left[\mathbf{U}|\mathbf{S}|^{\frac{1}{2}}\mathbf{W}_2 - \mathbf{U}|\mathbf{S}|^{\frac{1}{2}}\mathbf{U}^\top \mathbf{U}_2 \right]}_{\mathbf{T}_4} \\ &\quad + \underbrace{\left[\mathbf{U}|\mathbf{S}|^{\frac{1}{2}}\mathbf{U}^\top \mathbf{U}_2 - \mathbf{U}\mathbf{U}^\top \mathbf{U}_2|\mathbf{S}_2|^{\frac{1}{2}} \right]}_{\mathbf{T}_5} \\ &\quad + \underbrace{\left[\mathbf{U}\mathbf{U}^\top \mathbf{U}_2|\mathbf{S}_2|^{\frac{1}{2}} - \mathbf{U}_2|\mathbf{S}_2|^{\frac{1}{2}} \right]}_{\mathbf{T}_6}. \end{aligned} \tag{3}$$

We use the following Lemma 1,2 to bound the $\mathbf{T}_2, \mathbf{T}_3, \mathbf{T}_4$, and \mathbf{T}_5 and get

$$\|\mathbf{T}_2 + \mathbf{T}_3 + \mathbf{T}_4 + \mathbf{T}_5\|_{2 \rightarrow \infty} = O_p(n^{-1} \gamma^{-1/2}).$$

We use the following Lemma 3 to bound the \mathbf{T}_1 , and \mathbf{T}_6 and get

$$\|\mathbf{T}_1 + \mathbf{T}_6\|_{2 \rightarrow \infty} = (1 - \rho)^{1/2} \cdot O_p(n^{-1/2}) + O_p((\log n)^{2c} n^{-1} \gamma^{-1/2}),$$

for some constant c . Theorem 1 then follows immediately.

Lemma 1. For the term $\mathbf{T}_2, \mathbf{T}_5$ in Eq.(3), we have

$$\|\mathbf{T}_2\|_{2 \rightarrow \infty} = O_p(n^{-1} \gamma^{-1/2}), \|\mathbf{T}_5\|_{2 \rightarrow \infty} = O_p(n^{-1} \gamma^{-1/2}).$$

Proof. We first bound $\|\mathbf{T}_2\|_{2 \rightarrow \infty}$.

$$\begin{aligned}\|\mathbf{T}_2\|_{2 \rightarrow \infty} &\leq \|\mathbf{U}\|_{2 \rightarrow \infty} \cdot \left\| \mathbf{U}^\top \mathbf{U}_1 |\mathbf{S}_1|^{\frac{1}{2}} - |\mathbf{S}|^{\frac{1}{2}} \mathbf{U}^\top \mathbf{U}_1 \right\|_2 \cdot \|\mathbf{W}_1^\top \mathbf{W}_2\|_2 \\ &\leq \|\mathbf{U}\|_{2 \rightarrow \infty} \cdot \left\| \mathbf{U}^\top \mathbf{U}_1 |\mathbf{S}_1|^{\frac{1}{2}} - |\mathbf{S}|^{\frac{1}{2}} \mathbf{U}^\top \mathbf{U}_1 \right\|_2.\end{aligned}$$

For the first part, $\|\mathbf{U}\|_{2 \rightarrow \infty} = O_p(n^{-1/2})$. For the second part, we notice entry ij of it can be written as, $\forall i, j = 1, \dots, d$,

$$(\mathbf{U}^\top \mathbf{U}_1 |\mathbf{S}_1|^{\frac{1}{2}} - |\mathbf{S}|^{\frac{1}{2}} \mathbf{U}^\top \mathbf{U}_1)_{i,j} = [\mathbf{U}^\top \mathbf{U}_1]_{i,j} \cdot \left(\sqrt{|\lambda_j(\mathbf{A}_1)|} - \sqrt{|\lambda_i(\mathbf{P})|} \right).$$

So for $i \leq p, j \leq p$,

$$\begin{aligned}(\mathbf{U}^\top \mathbf{U}_1 |\mathbf{S}_1|^{\frac{1}{2}} - |\mathbf{S}|^{\frac{1}{2}} \mathbf{U}^\top \mathbf{U}_1)_{i,j} &= [\mathbf{U}^\top \mathbf{U}_1]_{i,j} \cdot \left(\sqrt{\lambda_j(\mathbf{A}_1)} - \sqrt{\lambda_i(\mathbf{P})} \right) \\ &= [\mathbf{U}^\top \mathbf{U}_1]_{i,j} \cdot (\lambda_j(\mathbf{A}_1) - \lambda_i(\mathbf{P})) \cdot \left(\sqrt{\lambda_j(\mathbf{A}_1)} + \sqrt{\lambda_i(\mathbf{P})} \right)^{-1}.\end{aligned}$$

Similarly, we have for $i > p, j > p$,

$$(\mathbf{U}^\top \mathbf{U}_1 |\mathbf{S}_1|^{\frac{1}{2}} - |\mathbf{S}|^{\frac{1}{2}} \mathbf{U}^\top \mathbf{U}_1)_{i,j} = [\mathbf{U}^\top \mathbf{U}_1]_{i,j} \cdot (\lambda_j(\mathbf{A}_1) - \lambda_i(\mathbf{P})) \cdot \left(-\sqrt{-\lambda_j(\mathbf{A}_1)} - \sqrt{-\lambda_i(\mathbf{P})} \right)^{-1}.$$

For $i > p, j \leq p$,

$$\begin{aligned}(\mathbf{U}^\top \mathbf{U}_1 |\mathbf{S}_1|^{\frac{1}{2}} - |\mathbf{S}|^{\frac{1}{2}} \mathbf{U}^\top \mathbf{U}_1)_{i,j} &= [\mathbf{U}^\top \mathbf{U}_1]_{i,j} \cdot (\lambda_j(\mathbf{A}_1) - \lambda_i(\mathbf{P})) \cdot \left(\sqrt{\lambda_j(\mathbf{A}_1)} + \sqrt{-\lambda_i(\mathbf{P})} \right)^{-1} \\ &\quad + 2 [\mathbf{U}^\top \mathbf{U}_1]_{i,j} \cdot \lambda_i(\mathbf{P}) \cdot \left(\sqrt{\lambda_j(\mathbf{A}_1)} + \sqrt{-\lambda_i(\mathbf{P})} \right)^{-1}.\end{aligned}$$

For $i \leq p, j > p$,

$$\begin{aligned}(\mathbf{U}^\top \mathbf{U}_1 |\mathbf{S}_1|^{\frac{1}{2}} - |\mathbf{S}|^{\frac{1}{2}} \mathbf{U}^\top \mathbf{U}_1)_{i,j} &= [\mathbf{U}^\top \mathbf{U}_1]_{i,j} \cdot (\lambda_j(\mathbf{A}_1) - \lambda_i(\mathbf{P})) \cdot \left(-\sqrt{-\lambda_j(\mathbf{A}_1)} - \sqrt{\lambda_i(\mathbf{P})} \right)^{-1} \\ &\quad - 2 [\mathbf{U}^\top \mathbf{U}_1]_{i,j} \cdot \lambda_i(\mathbf{P}) \cdot \left(\sqrt{-\lambda_j(\mathbf{A}_1)} + \sqrt{\lambda_i(\mathbf{P})} \right)^{-1}.\end{aligned}$$

We define matrices $\mathbf{H}_1, \mathbf{H}_2 \in \mathbb{R}^{d \times d}$ as

$$\begin{aligned}(\mathbf{H}_1)_{i,j} &= \left(\sqrt{|\lambda_j(\mathbf{A}_1)|} + \sqrt{|\lambda_i(\mathbf{P})|} \right)^{-1} \cdot \mathbb{I}(j \leq p) + \left(-\sqrt{|\lambda_j(\mathbf{A}_1)|} - \sqrt{|\lambda_i(\mathbf{P})|} \right)^{-1} \cdot \mathbb{I}(j > p), \\ (\mathbf{H}_2)_{i,j} &= \lambda_i(\mathbf{P}) \cdot \left(\sqrt{|\lambda_j(\mathbf{A}_1)|} + \sqrt{|\lambda_i(\mathbf{P})|} \right)^{-1}.\end{aligned}$$

According to Lemma 4, $\lambda_i(\mathbf{A}_1), \lambda_j(\mathbf{P}) = O_p(n\gamma), \Omega(n\gamma)$, it follows that

$$(\mathbf{H}_1)_{i,j} = O_p\left(\frac{1}{\sqrt{n\gamma}}\right), (\mathbf{H}_2)_{i,j} = O_p(\sqrt{n\gamma}).$$

Letting \circ denote the Hadamard matrix product, we arrive at the decomposition

$$\mathbf{U}^\top \mathbf{U}_1 |\mathbf{S}_1|^{\frac{1}{2}} - |\mathbf{S}|^{\frac{1}{2}} \mathbf{U}^\top \mathbf{U}_1 = (\mathbf{U}^\top \mathbf{U}_1 \mathbf{S}_1 - \mathbf{S} \mathbf{U}^\top \mathbf{U}_1) \circ \mathbf{H}_1 + \mathbf{V} \circ \mathbf{H}_2. \quad (4)$$

where $\mathbf{V} = \begin{pmatrix} 0 & -2\mathbf{U}_{(+)}^\top \mathbf{U}_{1(-)} \\ 2\mathbf{U}_{(-)}^\top \mathbf{U}_{1(+)} & 0 \end{pmatrix}$. The definition of $\mathbf{U}_{(+)}, \mathbf{U}_{(-)}, \mathbf{U}_{1(+)}, \mathbf{U}_{1(-)}$ can be found in Lemma 9, and from the proof of Lemma 9, we know $\|\mathbf{U}_{(+)}^\top \mathbf{U}_{1(-)}\|_F = O_p\left(\frac{1}{n\gamma}\right)$, $\|\mathbf{U}_{(-)}^\top \mathbf{U}_{1(+)}\|_F = O_p\left(\frac{1}{n\gamma}\right)$, So $\|\mathbf{V}\|_F = O_p\left(\frac{1}{n\gamma}\right)$. We thus have

$$\|\mathbf{V} \circ \mathbf{H}_2\|_2 \leq d \cdot \|\mathbf{H}_2\|_{\max} \cdot \|\mathbf{V}\|_F = O_p(\sqrt{n\gamma}) \cdot O_p\left(\frac{1}{n\gamma}\right) = O_p\left(\frac{1}{\sqrt{n\gamma}}\right).$$

And according to Lemma 5, $\|\mathbf{U}^\top \mathbf{U}_1 \mathbf{S}_1 - \mathbf{S} \mathbf{U}^\top \mathbf{U}_1\|_F = O_p(1)$. We thus have

$$\|(\mathbf{U}^\top \mathbf{U}_1 \mathbf{S}_1 - \mathbf{S} \mathbf{U}^\top \mathbf{U}_1) \circ \mathbf{H}_1\|_2 \leq d \cdot \|\mathbf{H}_1\|_{\max} \cdot \|\mathbf{U}^\top \mathbf{U}_1 \mathbf{S}_1 - \mathbf{S} \mathbf{U}^\top \mathbf{U}_1\|_F = O_p\left(\frac{1}{\sqrt{n\gamma}}\right) \cdot O_p(1) = O_p\left(\frac{1}{\sqrt{n\gamma}}\right).$$

So we finally bound $\mathbf{U}^\top \mathbf{U}_1 |\mathbf{S}_1|^{\frac{1}{2}} - |\mathbf{S}|^{\frac{1}{2}} \mathbf{U}^\top \mathbf{U}_1$ as

$$\|\mathbf{U}^\top \mathbf{U}_1 |\mathbf{S}_1|^{\frac{1}{2}} - |\mathbf{S}|^{\frac{1}{2}} \mathbf{U}^\top \mathbf{U}_1\|_2 = O_p\left(\frac{1}{\sqrt{n\gamma}}\right).$$

We therefore conclude

$$\|\mathbf{T}_2\|_{2 \rightarrow \infty} \leq O_p\left(\frac{1}{\sqrt{n}}\right) \cdot O_p\left(\frac{1}{\sqrt{n\gamma}}\right) = O_p\left(\frac{1}{n\sqrt{\gamma}}\right).$$

The proof for $\|\mathbf{T}_5\|_{2 \rightarrow \infty}$ is almost the same.

□

Lemma 2. For the term $\mathbf{T}_3, \mathbf{T}_4$ in Eq. (3), we have

$$\|\mathbf{T}_3\|_{2 \rightarrow \infty} = O_p(n^{-1}\gamma^{-1/2}), \|\mathbf{T}_4\|_{2 \rightarrow \infty} = O_p(n^{-1}\gamma^{-1/2}).$$

Proof. We first bound $\|\mathbf{T}_3\|_{2 \rightarrow \infty}$.

$$\begin{aligned} \|\mathbf{T}_3\|_{2 \rightarrow \infty} &\leq \|\mathbf{U}\|_{2 \rightarrow \infty} \cdot \|\mathbf{S}^{\frac{1}{2}}\|_2 \cdot \|\mathbf{U}^\top \mathbf{U}_1 - \mathbf{W}_1\|_2 \cdot \|\mathbf{W}_1^\top \mathbf{W}_2\|_2 \\ &\leq \|\mathbf{U}\|_{2 \rightarrow \infty} \cdot \|\mathbf{S}^{\frac{1}{2}}\|_2 \cdot \|\mathbf{U}^\top \mathbf{U}_1 - \mathbf{W}_1\|_2. \end{aligned}$$

Now $\|\mathbf{U}\|_{2 \rightarrow \infty} = O_p(n^{-1/2})$. $\| |\mathbf{S}|^{\frac{1}{2}} \|_2 = (\| |\mathbf{S}| \|_2)^{\frac{1}{2}} = (\|\mathbf{P}\|_2)^{\frac{1}{2}}$ and Lemma 4 implies $\|\mathbf{P}\|_2 = O_p(n\gamma)$. We thus have $\| |\mathbf{S}|^{\frac{1}{2}} \|_2 = O_p(\sqrt{n\gamma})$. And according to Lemma 9, $\|\mathbf{U}^\top \mathbf{U}_1 - \mathbf{W}_1\|_2 = O_p\left(\frac{1}{n\gamma}\right)$. We immediately conclude

$$\|\mathbf{T}_3\|_{2 \rightarrow \infty} = O_p\left(\frac{1}{n\sqrt{\gamma}}\right).$$

The proof for $\|\mathbf{T}_4\|_{2 \rightarrow \infty}$ is almost the same. □

Lemma 3. For the term $\mathbf{T}_1, \mathbf{T}_6$ in Eq.(3), we have

$$\|\mathbf{T}_1 + \mathbf{T}_6\|_{2 \rightarrow \infty} = (1 - \rho)^{1/2} \cdot O_p(n^{-1/2}) + O_p((\log n)^{2c} n^{-1} \gamma^{-1/2})$$

for some constant c .

Proof. According to B.2.4 in [Rubin-Delanchy et al. \(2017\)](#),

$$\mathbf{U}_1 |\mathbf{S}_1|^{\frac{1}{2}} = \mathbf{U} |\mathbf{S}|^{\frac{1}{2}} \mathbf{W}_1 + (\mathbf{A}_1 - \mathbf{P}) \mathbf{U} |\mathbf{S}|^{-\frac{1}{2}} \mathbf{W}_1 \mathbf{I}_{p,q} + \mathbf{R}_1,$$

for some (residual) matrix $\mathbf{R}_1 \in \mathbb{R}^{n \times d}$ satisfying $\|\mathbf{R}_1\|_{2 \rightarrow \infty} = O_p\left(\frac{(\log n)^{2c_1}}{n\gamma^{1/2}}\right)$ for some constant $c_1 > 0$. And we notice that $(\mathbf{I} - \mathbf{U}\mathbf{U}^\top)\mathbf{U} = 0$, then

$$\begin{aligned} \mathbf{T}_1 &= (\mathbf{I} - \mathbf{U}\mathbf{U}^\top) \mathbf{U}_1 |\mathbf{S}_1|^{\frac{1}{2}} \mathbf{W}_1^\top \mathbf{W}_2 \\ &= (\mathbf{I} - \mathbf{U}\mathbf{U}^\top) (\mathbf{A}_1 - \mathbf{P}) \mathbf{U} |\mathbf{S}|^{-\frac{1}{2}} \mathbf{W}_1 \mathbf{I}_{p,q} \mathbf{W}_1^\top \mathbf{W}_2 + (\mathbf{I} - \mathbf{U}\mathbf{U}^\top) \mathbf{R}_1 \mathbf{W}_1^\top \mathbf{W}_2 \\ &= (\mathbf{I} - \mathbf{U}\mathbf{U}^\top) (\mathbf{A}_1 - \mathbf{P}) \mathbf{U} |\mathbf{S}|^{-\frac{1}{2}} \mathbf{W}_2 \mathbf{I}_{p,q} + (\mathbf{I} - \mathbf{U}\mathbf{U}^\top) \mathbf{R}_1 \mathbf{W}_1^\top \mathbf{W}_2. \end{aligned}$$

With the similar proof, we have

$$\mathbf{T}_6 = -(\mathbf{I} - \mathbf{U}\mathbf{U}^\top) (\mathbf{A}_2 - \mathbf{P}) \mathbf{U} |\mathbf{S}|^{-\frac{1}{2}} \mathbf{W}_2 \mathbf{I}_{p,q} - (\mathbf{I} - \mathbf{U}\mathbf{U}^\top) \mathbf{R}_2.$$

We set $\mathbf{E} = \mathbf{A}_1 - \mathbf{A}_2$. We therefore have

$$\mathbf{T}_1 + \mathbf{T}_6 = (\mathbf{I} - \mathbf{U}\mathbf{U}^\top) \mathbf{E} \mathbf{U} |\mathbf{S}|^{-\frac{1}{2}} \mathbf{W}_2 \mathbf{I}_{p,q} + \mathbf{R},$$

where

$$\mathbf{R} = \mathbf{R}_1 \mathbf{W}_1^\top \mathbf{W}_2 - \mathbf{U}\mathbf{U}^\top \mathbf{R}_1 \mathbf{W}_1^\top \mathbf{W}_2 - \mathbf{R}_2 + \mathbf{U}\mathbf{U}^\top \mathbf{R}_2.$$

For the terms in \mathbf{R} ,

$$\begin{aligned}\|\mathbf{U}\mathbf{U}^\top \mathbf{R}_1 \mathbf{W}_1^\top \mathbf{W}_2\|_{2 \rightarrow \infty} &\leq \|\mathbf{U}\mathbf{U}^\top\|_\infty \cdot \|\mathbf{R}_1\|_{2 \rightarrow \infty} \cdot \|\mathbf{W}_1^\top \mathbf{W}_2\|_2 \\ &\leq O_p(1) \cdot O_p\left(\frac{(\log n)^{2c_1}}{n\gamma^{1/2}}\right) \cdot 1 \\ &= O_p\left(\frac{(\log n)^{2c_1}}{n\gamma^{1/2}}\right).\end{aligned}$$

With the similar proof, we have $\|\mathbf{R}_1 \mathbf{W}_1^\top \mathbf{W}_2\|_{2 \rightarrow \infty} = O_p\left(\frac{(\log n)^{2c_1}}{n\gamma^{1/2}}\right)$ and $\|\mathbf{U}\mathbf{U}^\top \mathbf{R}_1 \mathbf{W}_1^\top \mathbf{W}_2 - \mathbf{R}_2\|_{2 \rightarrow \infty}, \|\mathbf{U}\mathbf{U}^\top \mathbf{R}_2\|_{2 \rightarrow \infty} = O_p\left(\frac{(\log n)^{2c_2}}{n\gamma^{1/2}}\right)$. We thus have for some constant $c = \max\{c_1, c_2\}$,

$$\|\mathbf{R}\|_{2 \rightarrow \infty} = O_p\left(\frac{(\log n)^{2c}}{n\gamma^{1/2}}\right)$$

Now we bound the main part of $\mathbf{T}_1 + \mathbf{T}_6$,

$$\|(\mathbf{I} - \mathbf{U}\mathbf{U}^\top) \mathbf{E}\mathbf{U}|\mathbf{S}|^{-\frac{1}{2}} \mathbf{W}_2 \mathbf{I}_{p,q}\|_{2 \rightarrow \infty} \leq \|\mathbf{E}\mathbf{U}|\mathbf{S}|^{-\frac{1}{2}} \mathbf{W}_2 \mathbf{I}_{p,q}\|_{2 \rightarrow \infty} + \|\mathbf{U}\mathbf{U}^\top \mathbf{E}\mathbf{U}|\mathbf{S}|^{-\frac{1}{2}} \mathbf{W}_2 \mathbf{I}_{p,q}\|_{2 \rightarrow \infty}.$$

According to Lemma 6, we have $\|\mathbf{E}\mathbf{U}\|_{2 \rightarrow \infty} = \sqrt{1-\rho} \cdot O_p(\sqrt{\gamma}), \|\mathbf{U}^\top \mathbf{E}\mathbf{U}\|_F = \sqrt{1-\rho} \cdot O_p(\sqrt{\gamma})$. Thus

$$\begin{aligned}\|\mathbf{E}\mathbf{U}|\mathbf{S}|^{-\frac{1}{2}} \mathbf{W}_2 \mathbf{I}_{p,q}\|_{2 \rightarrow \infty} &\leq \|\mathbf{E}\mathbf{U}\|_{2 \rightarrow \infty} \cdot \|\mathbf{S}\|_2^{-\frac{1}{2}} \cdot \|\mathbf{W}_2 \mathbf{I}_{p,q}\|_2 \\ &\leq \sqrt{1-\rho} \cdot O_p(\sqrt{\gamma}) \cdot O_p\left(\frac{1}{\sqrt{n\gamma}}\right) \cdot 1 \\ &= \sqrt{1-\rho} \cdot O_p\left(\frac{1}{\sqrt{n}}\right),\end{aligned}$$

$$\begin{aligned}\|\mathbf{U}\mathbf{U}^\top \mathbf{E}\mathbf{U}|\mathbf{S}|^{-\frac{1}{2}} \mathbf{W}_2 \mathbf{I}_{p,q}\|_{2 \rightarrow \infty} &\leq \|\mathbf{U}\|_{2 \rightarrow \infty} \cdot \|\mathbf{U}^\top \mathbf{E}\mathbf{U}\|_F \cdot \|\mathbf{S}\|_2^{-\frac{1}{2}} \cdot \|\mathbf{W}_2 \mathbf{I}_{p,q}\|_2 \\ &\leq O_p\left(\frac{1}{\sqrt{n}}\right) \cdot \sqrt{1-\rho} \cdot O_p(\sqrt{\gamma}) \cdot O_p\left(\frac{1}{\sqrt{n\gamma}}\right) \cdot 1 \\ &= \sqrt{1-\rho} \cdot O_p\left(\frac{1}{n}\right),\end{aligned}$$

We thus know the main part of $\mathbf{T}_1 + \mathbf{T}_6$ has the bound

$$\|(\mathbf{I} - \mathbf{U}\mathbf{U}^\top) \mathbf{E}\mathbf{U}|\mathbf{S}|^{-\frac{1}{2}} \mathbf{W}_2 \mathbf{I}_{p,q}\|_{2 \rightarrow \infty} = \sqrt{1-\rho} \cdot O_p\left(\frac{1}{\sqrt{n}}\right).$$

So

$$\|\mathbf{T}_1 + \mathbf{T}_6\|_{2 \rightarrow \infty} = \sqrt{1-\rho} \cdot O_p\left(\frac{1}{\sqrt{n}}\right) + O_p\left(\frac{(\log n)^{2c}}{n\gamma^{1/2}}\right).$$

□

Lemma 4. Let $|\lambda_1(\mathbf{A}_1)| \geq |\lambda_2(\mathbf{A}_1)| \geq \dots$ be the eigenvalues of \mathbf{A}_1 , ordered in decreasing modulus. We then have

$$\lambda_k(\mathbf{A}_1) = \begin{cases} \Omega_p(n\gamma), O_p(n\gamma) & \text{for } k = 1, 2, \dots, d \\ O_p(\sqrt{n\gamma}) & \text{for } k = d + 1, \dots, n \end{cases},$$

The same bounds are true for the eigenvalues of \mathbf{A}_2 . And for the eigenvalues of \mathbf{P} , we have

$$\lambda_k(\mathbf{P}) = \begin{cases} \Omega(n\gamma), O_p(n\gamma) & \text{for } k = 1, 2, \dots, d \\ 0 & \text{for } k = d + 1, \dots, n \end{cases}.$$

Proof. Recall the assumption on the maximum expected degree of \mathbf{P} , i.e.,

$$\max_{1 \leq i \leq n} \sum_{j=1}^n \mathbf{P}_{i,j} \geq \max_{1 \leq i \leq n} \sum_{j=1}^n \mathbf{P}_{i,j}(1 - \mathbf{P}_{i,j}) \geq C \ln^4 n.$$

We then have, from Theorem 1 in [Lu and Peng \(2013\)](#) and Weyl's inequality, that

$$\begin{aligned} \max_{k=1,2,\dots,n} |\lambda_k(\mathbf{A}_1) - \lambda_k(\mathbf{P})| &\leq \|\mathbf{A}_1 - \mathbf{P}\|_2 \\ &\leq [2 + o(1)] \sqrt{\max_{1 \leq i \leq n} \sum_{j=1}^n \mathbf{P}_{i,j}} = O_p(\sqrt{n\gamma}). \end{aligned} \tag{5}$$

Since \mathbf{P} is symmetric and $\text{rank}(\mathbf{P}) = d$, there exists a decomposition $\mathbf{P} = \gamma \mathbf{X} \mathbf{I}_{p,q} \mathbf{X}^\top$, where $\mathbf{X} \in \mathbb{R}^{n \times d}$ and each row of \mathbf{X} corresponds the latent position of each vertex in G_1 , and $\mathbf{I}_{p,q} = \text{diag}(1, \dots, 1, -1, \dots, -1)$ with p ones followed by q minus ones on its diagonal satisfying $p + q = d$. We now consider the eigenvalues of \mathbf{P} . As \mathbf{P} is rank d , we have $\lambda_k(\mathbf{P}) = 0$ for $k > d$. Furthermore, for $k = 1, \dots, d$

$$\lambda_k(\mathbf{P}) = \lambda_k(\gamma \mathbf{X} \mathbf{I}_{p,q} \mathbf{X}^\top) = \gamma \lambda_k(\mathbf{X}^\top \mathbf{X} \mathbf{I}_{p,q}) = n\gamma \cdot \lambda_k\left(\frac{1}{n} \sum_{i=1}^n X_i X_i^\top \mathbf{I}_{p,q}\right),$$

where X_i represents the i th row of \mathbf{X} , i.e., the latent position of i th vertex. Since $\frac{1}{n} \sum_{i=1}^n X_i X_i^\top \mathbf{I}_{p,q}$ converges to a constant matrix, we have

$$\lambda_k(\mathbf{P}) = \begin{cases} \Omega(n\gamma), O_p(n\gamma) & \text{for } k = 1, 2, \dots, d \\ 0 & \text{for } k \geq d + 1 \end{cases}.$$

Eq. (5) then implies

$$\lambda_k(\mathbf{A}_1) = \begin{cases} \Omega(n\gamma), O_p(n\gamma) & \text{for } k = 1, \dots, d \\ O_p(\sqrt{n\gamma}) & \text{for } k \geq d + 1 \end{cases}.$$

The proof for the eigenvalues of \mathbf{A}_2 is identical. □

Lemma 5. For the term in Eq. (4), we have

$$\|\mathbf{U}^\top \mathbf{U}_1 \mathbf{S}_1 - \mathbf{S} \mathbf{U}^\top \mathbf{U}_1\|_F = O_p(1).$$

Proof. Recalling the block spectral decomposition $\mathbf{A}_1 = \mathbf{U}_1 \mathbf{S}_1 \mathbf{U}_1^\top + \mathbf{U}'_1 \mathbf{S}'_1 \mathbf{U}'_1{}^\top$, we have $\mathbf{A}_1 \mathbf{U}_1 = \mathbf{U}_1 \mathbf{S}_1$. Similarly, we have $\mathbf{P} \mathbf{U} = \mathbf{U} \mathbf{S}$. Then

$$\mathbf{U}^\top \mathbf{U}_1 \mathbf{S}_1 - \mathbf{S} \mathbf{U}^\top \mathbf{U}_1 = \mathbf{U}^\top \mathbf{A}_1 \mathbf{U}_1 - \mathbf{U}^\top \mathbf{P} \mathbf{U}_1 = \mathbf{U}^\top (\mathbf{A}_1 - \mathbf{P}) \mathbf{U}_1.$$

And we split $\mathbf{U}^\top (\mathbf{A}_1 - \mathbf{P}) \mathbf{U}_1$ as

$$\mathbf{U}^\top (\mathbf{A}_1 - \mathbf{P}) \mathbf{U}_1 = \underbrace{\mathbf{U}^\top (\mathbf{A}_1 - \mathbf{P}) (\mathbf{I} - \mathbf{U} \mathbf{U}^\top) \mathbf{U}_1}_{\mathbf{Q}_1} + \underbrace{\mathbf{U}^\top (\mathbf{A}_1 - \mathbf{P}) \mathbf{U} \mathbf{U}^\top \mathbf{U}_1}_{\mathbf{Q}_2}.$$

Because

$$\|\mathbf{Q}_1\|_F \leq \|\mathbf{U}^\top (\mathbf{A}_1 - \mathbf{P})\|_2 \cdot \|(\mathbf{I} - \mathbf{U} \mathbf{U}^\top) \mathbf{U}_1\|_F,$$

$$\|\mathbf{Q}_2\|_F \leq \|\mathbf{U}^\top (\mathbf{A}_1 - \mathbf{P}) \mathbf{U}\|_F \cdot \|\mathbf{U}^\top \mathbf{U}_1\|_2 \leq \|\mathbf{U}^\top (\mathbf{A}_1 - \mathbf{P}) \mathbf{U}\|_F,$$

and according to Lemma 6 and Lemma 7, we have $\|\mathbf{U}^\top (\mathbf{A}_1 - \mathbf{P})\|_2 = O_p(\sqrt{n\gamma})$, $\|(\mathbf{I} - \mathbf{U} \mathbf{U}^\top) \mathbf{U}_1\|_F = O_p(\frac{1}{\sqrt{n\gamma}})$, $\|\mathbf{U}^\top (\mathbf{A}_1 - \mathbf{P}) \mathbf{U}\|_F = O_p(\sqrt{\gamma})$. Thus

$$\|\mathbf{U}^\top \mathbf{U}_1 \mathbf{S}_1 - \mathbf{S} \mathbf{U}^\top \mathbf{U}_1\|_F = \|\mathbf{U}^\top (\mathbf{A}_1 - \mathbf{P}) \mathbf{U}_1\|_F = O_p(1).$$

□

Lemma 6. Let $\mathbf{E} = \mathbf{A}_1 - \mathbf{A}_2$, then

$$\|\mathbf{E} \mathbf{U}\|_{2 \rightarrow \infty} = \sqrt{1 - \rho} \cdot O_p(\sqrt{\gamma}), \|\mathbf{E} \mathbf{U}\|_2 = \sqrt{1 - \rho} \cdot O_p(\sqrt{n\gamma}),$$

and

$$\|\mathbf{U}^\top \mathbf{E} \mathbf{U}\|_F = \sqrt{1 - \rho} \cdot O_p(\sqrt{\gamma}).$$

For $\mathbf{A}_1 - \mathbf{P}$ and $\mathbf{A}_2 - \mathbf{P}$, we have the same results but without $\sqrt{1 - \rho}$.

Proof. For $\mathbf{U}^\top \mathbf{E} \mathbf{U}$, we note that the ij th element of $\mathbf{U}^\top \mathbf{E} \mathbf{U}$ is of the form

$$(\mathbf{U}^\top \mathbf{E} \mathbf{U})_{i,j} = \sum_{k < l} 2 \mathbf{U}_{k,i} \mathbf{E}_{k,l} \mathbf{U}_{l,j} + \sum_k \mathbf{U}_{k,i} \mathbf{E}_{k,k} \mathbf{U}_{k,j},$$

which is a sum of *independent* mean 0 random variables, and hence, by Bernstein's inequality

$$(\mathbf{U}^\top \mathbf{E} \mathbf{U})_{i,j} = \sqrt{1-\rho} \cdot O_p(\sqrt{\gamma}).$$

Since $(\mathbf{U}^\top \mathbf{E} \mathbf{U})$ is a $d \times d$ matrix where d is fixed with n , we have, by a union bound

$$\|\mathbf{U}^\top \mathbf{E} \mathbf{U}\|_F = \sqrt{1-\rho} \cdot O_p(\sqrt{\gamma}).$$

For $\mathbf{E} \mathbf{U}$, we notice

$$\|\mathbf{E} \mathbf{U}\|_2 \leq \sqrt{n} \cdot \|\mathbf{E} \mathbf{U}\|_{2 \rightarrow \infty} = \sqrt{n} \cdot \max_{1 \leq i \leq n} \|(\mathbf{E} \mathbf{U})_i\|_2 = \sqrt{n} \cdot \max_{1 \leq i \leq n} \sqrt{\sum_{j=1}^d (\mathbf{E} \mathbf{U})_{i,j}^2},$$

where $(\mathbf{E} \mathbf{U})_i$ represents the i th row of $(\mathbf{E} \mathbf{U})$, and by Bernstein's inequality

$$(\mathbf{E} \mathbf{U})_{i,j} = \sqrt{1-\rho} \cdot O_p(\sqrt{\gamma})$$

. Then

$$\|\mathbf{E} \mathbf{U}\|_{2 \rightarrow \infty} = \sqrt{1-\rho} \cdot O_p(\sqrt{\gamma}), \|\mathbf{E} \mathbf{U}\|_2 = \sqrt{1-\rho} \cdot O_p(\sqrt{n\gamma}).$$

For $\mathbf{A}_1 - \mathbf{P}$ and $\mathbf{A}_2 - \mathbf{P}$, the proof is similar. □

Lemma 7. For terms $\mathbf{U}, \mathbf{U}_1, \mathbf{U}_2$ in the block spectral decompositions of $\mathbf{P}, \mathbf{A}_1, \mathbf{A}_2$, we have

$$\begin{aligned} \|(\mathbf{I} - \mathbf{U} \mathbf{U}^\top) \mathbf{U}_1\|_F &= O_p\left(\frac{1}{\sqrt{n\gamma}}\right), \|(\mathbf{I} - \mathbf{U} \mathbf{U}^\top) \mathbf{U}_2\|_F = O_p\left(\frac{1}{\sqrt{n\gamma}}\right), \\ \|(\mathbf{U}_1 \mathbf{U}_1^\top - \mathbf{I}) \mathbf{U}_2\|_F &= \sqrt{1-\rho} \cdot O_p\left(\frac{1}{\sqrt{n\gamma}}\right). \end{aligned}$$

Proof. By applying Theorem 2 in [Yu et al. \(2014\)](#), we have

$$\arg \min_{\mathbf{O} \in \mathbb{O}_d} \|\mathbf{U}_1 - \mathbf{U} \mathbf{O}\|_F \leq \frac{2^{3/2} \cdot d^{1/2} \cdot \|\mathbf{A}_1 - \mathbf{P}\|_2}{\lambda_d(\mathbf{P}) - \lambda_{(d+1)}(\mathbf{P})},$$

According to Lemma 4 and Lemma 8, we have

$$\lambda_d(\mathbf{P}) = \Omega(n\gamma), \lambda_{(d+1)}(\mathbf{P}) = 0, \|\mathbf{A}_1 - \mathbf{P}\|_2 = O_p(\sqrt{n\gamma}).$$

Thus $\arg \min_{\mathbf{O} \in \mathbb{O}_d} \|\mathbf{U}_1 - \mathbf{U}\mathbf{O}\|_F = O_p\left(\frac{1}{\sqrt{n\gamma}}\right)$. We therefore have

$$\begin{aligned} \|(\mathbf{I} - \mathbf{U}\mathbf{U}^\top) \mathbf{U}_1\|_F &= \|\mathbf{U}_1 - \mathbf{U}(\mathbf{U}^\top \mathbf{U}_1)\|_F = \arg \min_{\mathbf{T}} \|\mathbf{U}_1 - \mathbf{U}\mathbf{T}\|_F \\ &\leq \arg \min_{\mathbf{O} \in \mathbb{O}_d} \|\mathbf{U}_1 - \mathbf{U}\mathbf{O}\|_F = O_p\left(\frac{1}{\sqrt{n\gamma}}\right). \end{aligned}$$

The proof for $(\mathbf{I} - \mathbf{U}\mathbf{U}^\top) \mathbf{U}_2$ is identical.

And according to Lemma 8, $\|\mathbf{E}\|_2 = \sqrt{1 - \rho} \cdot O_p(\sqrt{n\gamma})$. Then with the similar proof, we have $\|(\mathbf{U}_1 \mathbf{U}_1^\top - \mathbf{I}) \mathbf{U}_2\|_F = \sqrt{1 - \rho} \cdot O_p\left(\frac{1}{\sqrt{n\gamma}}\right)$.

□

Lemma 8. Let $\mathbf{E} = \mathbf{A}_1 - \mathbf{A}_2$, then

$$\|\mathbf{E}\|_2 = \sqrt{1 - \rho} \cdot O_p(\sqrt{n\gamma}).$$

And similarly, we have

$$\|\mathbf{A}_1 - \mathbf{P}\|_2 = O_p(\sqrt{n\gamma}), \|\mathbf{A}_2 - \mathbf{P}\|_2 = O_p(\sqrt{n\gamma}).$$

Proof. Recall that $\mathbf{E}_{ij} = \mathbf{A}_{1,ij} - \mathbf{A}_{2,ij}$ where $\mathbf{A}_{1,ij}$ and $\mathbf{A}_{2,ij}$ are ρ -correlated Bernoulli random variables. We thus have $\text{Var}[\mathbf{E}_{i,j}] = 2\mathbf{P}_{i,j}(1 - \mathbf{P}_{i,j})(1 - \rho)$. Furthermore, according to our assumption,

$$\max_{1 \leq i \leq n} \sum_{j=1}^n \text{Var}[\mathbf{E}_{i,j}] = 2(1 - \rho) \max_{1 \leq i \leq n} \sum_{j=1}^n \mathbf{P}_{i,j}(1 - \mathbf{P}_{i,j}) \geq 2(1 - \rho) \cdot C \log^4 n.$$

On the other hand, because X_i magnitude does not change with n , $\mathbf{P}_{i,j} = \gamma \cdot X_i \mathbf{I}_{p,q} X_j^\top = O_p(\gamma)$. We therefore have $\max_{1 \leq i \leq n} \sum_{j=1}^n \text{Var}[\mathbf{E}_{i,j}] = (1 - \rho) \cdot O_p(n\gamma)$. Applying Theorem 7 in Lu and Peng (2013) yields the stated claim. The proof for $\|\mathbf{A}_1 - \mathbf{P}\|_2, \|\mathbf{A}_2 - \mathbf{P}\|_2$ is similar. □

Lemma 9. With proper setting of $\mathbf{W}_1, \mathbf{W}_2$, we can bound $\mathbf{U}^\top \mathbf{U}_1 - \mathbf{W}_1, \mathbf{U}^\top \mathbf{U}_2 - \mathbf{W}_2$ as

$$\|\mathbf{U}^\top \mathbf{U}_1 - \mathbf{W}_1\|_F = O_p\left(\frac{1}{n\gamma}\right), \|\mathbf{U}^\top \mathbf{U}_2 - \mathbf{W}_2\|_F = O_p\left(\frac{1}{n\gamma}\right).$$

Proof. Without loss of generality, we let $\mathbf{U}_1 = [\mathbf{U}_{1(+)} | \mathbf{U}_{1(-)}]$ such that the columns of $\mathbf{U}_{1(+)}$ and $\mathbf{U}_{1(-)}$ consist of orthonormal eigenvectors corresponding to the largest p positive

and q negative non-zero eigenvalues of \mathbf{A}_1 , respectively. Similarly, we set $\mathbf{U} = [\mathbf{U}_{(+)} | \mathbf{U}_{(-)}]$.

We therefore have

$$\mathbf{U}^\top \mathbf{U}_1 = \begin{pmatrix} \mathbf{U}_{(+)}^\top \mathbf{U}_{1(+)} & \mathbf{U}_{(+)}^\top \mathbf{U}_{1(-)} \\ \mathbf{U}_{(-)}^\top \mathbf{U}_{1(+)} & \mathbf{U}_{(-)}^\top \mathbf{U}_{1(-)} \end{pmatrix} \in \mathbb{R}^{d \times d}.$$

Let $\mathbf{U}_{(+)}^\top \mathbf{U}_{1(+)} = \mathbf{V}_{(+)} \mathbf{\Lambda}_{(+)} \mathbf{V}_{(+)}^\top$ be the singular value decomposition of $\mathbf{U}_{(+)}^\top \mathbf{U}_{1(+)} \in \mathbb{R}^{p \times p}$ and define $\mathbf{W}_{1(+)} = \mathbf{V}_{(+)} \mathbf{V}_{(+)}^\top \in \mathbb{O}_p$. Similarly, define $\mathbf{W}_{1(-)} \in \mathbb{O}_q$ using the singular value decomposition of $\mathbf{U}_{(-)}^\top \mathbf{U}_{1(-)}$ and define \mathbf{W}_1 as the block-diagonal matrix

$$\mathbf{W}_1 = \begin{pmatrix} \mathbf{W}_{1(+)} & 0 \\ 0 & \mathbf{W}_{1(-)} \end{pmatrix} \in \mathbb{O}_d.$$

We now analyze each block of $\mathbf{U}^\top \mathbf{U}_1 - \mathbf{W}_1$. For the first diagonal block,

$$\begin{aligned} \|\mathbf{U}_{(+)}^\top \mathbf{U}_{1(+)} - \mathbf{W}_{1(+)}\|_F^2 &= \text{tr} \left[(\mathbf{U}_{(+)}^\top \mathbf{U}_{1(+)} - \mathbf{W}_{1(+)}) (\mathbf{U}_{(+)}^\top \mathbf{U}_{1(+)} - \mathbf{W}_{1(+)})^\top \right] \\ &= \text{tr} (\mathbf{\Lambda}_{(+)}^2 - 2\mathbf{\Lambda}_{(+)} + \mathbf{I}) \\ &= \sum_{i=1}^p (1 - \sigma_i)^2, \end{aligned}$$

where $\sigma_1, \dots, \sigma_p$ are the singular values of $\mathbf{U}_{(+)}^\top \mathbf{U}_{1(+)}$ and $\mathbf{\Lambda}_{(+)} = \text{diag}\{\sigma_1, \dots, \sigma_p\}$. Since $\mathbf{U}_{(+)}$ and $\mathbf{U}_{1(+)}$ both have orthonormal columns, $\|\mathbf{U}_{(+)}^\top \mathbf{U}_{1(+)}\|_2 \leq 1$ and hence, for all $i = 1, 2, \dots, p$,

$$0 \leq 1 - \sigma_i = \frac{1 - \sigma_i^2}{1 + \sigma_i} \leq 1 - \sigma_i^2$$

We therefore have

$$\sum_{i=1}^p (1 - \sigma_i)^2 \leq \sum_{i=1}^p (1 - \sigma_i^2)^2 \leq \left(\sum_{i=1}^p 1 - \sigma_i^2 \right)^2 \quad (6)$$

Recalling the relationship between the sin- Θ distance and singular values (see e.g., Lemma 1 in [Cai and Zhang \(2018\)](#)), we have

$$\sum_{i=1}^p (1 - \sigma_i^2) \leq \inf_{\mathbf{O} \in \mathbb{O}_p} \|\mathbf{U}_{(+)} - \mathbf{U}_{1(+)} \mathbf{O}\|_F^2.$$

Eq. (6) then implies

$$\|\mathbf{U}_{(+)}^\top \mathbf{U}_{1(+)} - \mathbf{W}_{1(+)}\|_F \leq \inf_{\mathbf{O} \in \mathbb{O}_p} \|\mathbf{U}_{(+)} - \mathbf{U}_{1(+)} \mathbf{O}\|_F^2.$$

By applying Theorem 2 in [Yu et al. \(2014\)](#), we have

$$\inf_{\mathbf{O} \in \mathbb{O}_p} \|\mathbf{U}_{(+)} - \mathbf{U}_{1(+)} \mathbf{O}\|_F \leq \frac{2^{3/2} \cdot d^{1/2} \cdot \|\mathbf{A}_1 - \mathbf{P}\|_2}{\lambda_{(+p)}(\mathbf{P})},$$

where $\lambda_{(+p)}(\mathbf{P})$ is the p -th largest positive eigenvalue of $\mathbf{P} = \mathbb{E}[\mathbf{A}_1]$. According to Lemma 4 and Lemma 8, we have

$$\lambda_{(+p)}(\mathbf{P}) = \Omega(n\gamma), \quad \|\mathbf{A}_1 - \mathbf{P}\|_2 = O_p(\sqrt{n\gamma}).$$

We therefore have

$$\begin{aligned} \inf_{\mathbf{O} \in \mathbb{O}_p} \|\mathbf{U}_{(+)} - \mathbf{U}_{1(+)} \mathbf{O}\|_F &= O_p\left(\frac{1}{\sqrt{n\gamma}}\right), \\ \|\mathbf{U}_{(+)}^\top \mathbf{U}_{1(+)} - \mathbf{W}_{1(+)}\|_F &= O_p\left(\frac{1}{n\gamma}\right). \end{aligned}$$

The same argument also yield $\|\mathbf{U}_{(-)}^\top \mathbf{U}_{1(-)} - \mathbf{W}_{1(-)}\|_F = O_p((n\gamma)^{-1})$.

We now bound $\mathbf{U}_{(+)}^\top \mathbf{U}_{1(-)}$. Let $u_{(+)}^i$ and $w_{1(-)}^j$ be the i th column of $\mathbf{U}_{(+)}$ and j th column of $\mathbf{U}_{1(-)}$, respectively. The ij -th entry of $\mathbf{U}_{(+)}^\top \mathbf{U}_{1(-)}$ is $(u_{(+)}^i)^\top w_{1(-)}^j$ and hence

$$(u_{(+)}^i)^\top w_{1(-)}^j = \frac{(u_{(+)}^i)^\top (\mathbf{P} - \mathbf{A}_1) w_{1(-)}^j}{\lambda_{(+i)}(\mathbf{P}) - \lambda_{(-j)}(\mathbf{A}_1)}$$

As the positive eigenvalues of \mathbf{P} are separated from the negative eigenvalues of \mathbf{A}_1 , we have, by Lemma 4, $[\lambda_{(+i)}(\mathbf{P}) - \lambda_{(-j)}(\mathbf{A}_1)]^{-1} = O_p((n\gamma)^{-1})$. Furthermore, since $(u_{(+)}^i)^\top (\mathbf{P} - \mathbf{A}_1) w_{1(-)}^j$ is the ij -th entry of $\mathbf{U}_{(+)}^\top (\mathbf{P} - \mathbf{A}_1) \mathbf{U}_{1(-)}$, we have

$$\|\mathbf{U}_{(+)}^\top \mathbf{U}_{1(-)}\|_F = O_p\left(\frac{1}{n\gamma}\right) \cdot \|\mathbf{U}_{(+)}^\top (\mathbf{P} - \mathbf{A}_1) \mathbf{U}_{1(-)}\|_F \leq O_p\left(\frac{1}{n\gamma}\right) \cdot \|\mathbf{U}^\top (\mathbf{P} - \mathbf{A}_1) \mathbf{U}_1\|_F.$$

Finally, in Lemma 1, we have proved $\|\mathbf{U}^\top (\mathbf{P} - \mathbf{A}_1) \mathbf{U}_1\|_F = O_p(1)$ and hence

$$\|\mathbf{U}_{(+)}^\top \mathbf{U}_{1(-)}\|_F = O_p\left(\frac{1}{n\gamma}\right).$$

An identical argument also yield $\|\mathbf{U}_{(-)}^\top \mathbf{U}_{1(+)}\|_F = O_p((n\gamma)^{-1})$. Combining the various blocks together yield

$$\|\mathbf{U}^\top \mathbf{U}_1 - \mathbf{W}_1\|_F = O_p\left(\frac{1}{n\gamma}\right).$$

The proof for $\|\mathbf{U}^\top \mathbf{U}_2 - \mathbf{W}_2\|_F$ is identical. □